JOURNAL OF NEUROPHYSIOLOGY
Vol. 72, No. 3, September 1994. *Printed in U.S.A.*

Synchronization Properties of Spindle Oscillations in a Thalamic Reticular Nucleus Model

DAVID GOLOMB, XIAO-JING WANG, AND JOHN RINZEL
Mathematical Research Branch, National Institute of Diabetes and Digestive and Kidney Diseases, National Institutes of Health, Bethesda, Maryland 20814; and Department of Mathematics, University of Pittsburgh, Pittsburgh, Pennsylvania 15260

SUMMARY AND CONCLUSIONS

1. We address the hypothesis of Steriade and colleagues that the thalamic reticular nucleus (RE) is a pacemaker for thalamocortical spindle oscillations by developing and analyzing a model of a large population of all-to-all coupled inhibitory RE neurons.

2. Each RE neuron has three ionic currents: a low-threshold T-type Ca^{2+} current ($I_{Ca\text{-}T}$), a calcium-activated potassium current (I_{AHP}) and a leakage current (I_L). $I_{Ca\text{-}T}$ underlies a cell's postinhibitory rebound properties, whereas I_{AHP} hyperpolarizes the neuron after a burst. Each neuron, which is a conditional oscillator, is coupled to all other RE neurons via fast γ-aminobutyric acid-A ($GABA_A$) and slow $GABA_B$ synapses.

3. For generating network oscillations I_{AHP} may not be necessary. Synaptic inhibition can provide the hyperpolarization for deinactivating $I_{Ca\text{-}T}$ that causes bursting if the reversal potentials for $GABA_A$ and $GABA_B$ synapses are sufficiently negative.

4. If model neurons display sufficiently powerful rebound excitability, an isolated RE network of such neurons oscillates with partial but typically not full synchrony. The neurons spontaneously segregate themselves into several macroscopic clusters. The neurons within a cluster follow the same time course, but the clusters oscillate differently from one another. In addition to activity patterns in which clusters burst sequentially (e.g., 2 or 3 clusters bursting alternately), a two-cluster state may occur with one cluster active and one quiescent. Because the neurons are all-to-all coupled, the cluster states do not have any spatial structure.

5. We have explored the sensitivity of such partially synchronized patterns to heterogeneity in cells' intrinsic properties and to simulated neuroelectric noise. Although either precludes precise clustering, modest levels of heterogeneity or noise lead to approximate clustering of active cells. The population-averaged voltage may oscillate almost regularly but individual cells burst at nearly every second cycle or less frequently. The active-quiescent state is not robust at all to heterogeneity or noise. Total asynchrony is observed when heterogeneity or noise is too large, e.g., even at 25% heterogeneity for our reference set of parameter values.

6. The fast $GABA_A$ inhibition (with a reversal potential more negative than, say, -65 mV) favors the cluster states and prevents full synchrony. Our simulation results suggest two mechanisms that can fully synchronize the isolated RE network model. With $GABA_A$ removed or almost totally blocked, $GABA_B$ inhibition (because it is slow) can lead to full synchrony, which is partially robust to heterogeneity and noise. A second possibility, also robust to heterogeneity and noise, is realized if the $GABA_A$ synapses have a less negative reversal potential and provide shunting rather than hyperpolarizing inhibition.

7. We examined the effects of fast excitation from thalamocortical (TC) cells. The TC output is generated by a synchronous TC pool that receives $GABA_A$ and $GABA_B$ inhibition from the RE network and sends back amino-3-hydroxy-5-methyl-4-isoxazolepropionic acid (AMPA)-mediated excitation. The TC pool has three ionic currents: $I_{Ca\text{-}T}$, I_L, and a hyperpolarization-activated cation ("sag") current, I_{sag}.

8. Modest excitation from the TC pool can eliminate cluster oscillations and synchronize fully the RE network, with robustness to heterogeneity and noise. Furthermore, strong AMPA excitation can create synchronized oscillations in cases where without it the RE system is at rest.

9. The oscillation frequency of the RE-TC network depends mainly on the GABA inhibition from the RE cells to the TC pool. Blocking $GABA_A$ decreases the frequency because of an indirect enhancement of the sag current in the TC pool, whereas blocking $GABA_B$ increases it.

INTRODUCTION

It is well known that the 7- to 14-Hz spindle brain waves, an electrographic landmark for the onset of sleep, originate in the thalamus (Steriade and Deschênes 1984; Steriade et al. 1990, 1993). According to Andersen (Andersen and Andersson 1968), recurrent synaptic inhibition plays an essential role in the synchronization of thalamic network spindle oscillations. More recent work by Steriade and colleagues identified a morphological substrate for providing this inhibitory synaptic organization, the thalamic reticular (RE) nucleus (Steriade et al. 1990). A thin neuronal sheet embracing partially the dorsal thalamus, the RE network consists of synaptically coupled GABAergic neurons (Deschênes et al. 1985; Houser et al. 1980; Montero and Singer 1984; Ohara and Lieberman 1985; Yen et al. 1985) that are capable of rhythmic bursting due to the presence of a T-type, low-threshold calcium current (Avanzini et al. 1989; Bal and McCormick 1993; Huguenard and Prince 1992; Llinás and Geijo-Barrientos 1988; Mulle et al. 1986; Shosaku et al. 1989). The RE cells receive axonal collaterals from the thalamocortical (TC) relay cells and project back to the relay nuclei with significant divergence. Furthermore, the TC cells also possess a T-type calcium current (Coulter et al. 1989; Deschênes et al. 1984; Jahnsen and Llinás 1984a,b) that endows them with the ability to fire rebound bursts of spikes in response to inhibitory postsynaptic potentials (IPSPs) of RE origin. It was found that spindles in thalamic nuclei could be abolished by depriving them of RE input (Steriade et al. 1985). Moreover, in a few nuclear groups that are not connected with the RE, spindle oscillations have never been observed (Mulle et al. 1985).

In vivo lesion experiments on cats showed that spindles could persist in an RE isolated from major afferents (Steriade et al. 1987), suggesting that the synaptic organization

within the RE nucleus alone is capable of giving rise to coherent rhythmic activities. On the other hand, recent experiments with a ferret in vitro slice preparation indicate that maintained spindle oscillations in RE require two-way interactions intact between RE neurons and TC neurons in the thalamus proper (von Krosigk et al. 1993a). These experiments therefore yielded important results about and provoked further interest in elucidating the respective roles in thalamic synchronization for the two possible mechanisms: the intrinsic RE circuitry and the RE-TC reciprocal connection.

The present work was designed specifically to address this issue using a computational approach. In a previous work regarding the synchronization of RE neurons, Wang and Rinzel (1992, 1993) have shown that mutual inhibition can synchronize neurons endowed with a rebound property under the condition that the postsynaptic conductance possesses a slow decay time constant. In these references the notion of synchrony was defined in the idealistic sense of phase-locking with zero phase difference. That is, every cell behaves in exactly the same way, and the network forms a giant cluster of dynamically identical oscillators. Golomb and Rinzel (1993, 1994a,b) simulated a large network of such model neurons and examined how the network's behavior depends on various biophysical parameters. The effects of variability in the cellular properties, e.g., the maximal conductance of the T-type Ca^{2+} channel, and the effects of time-dependent neuroelectric noise, were also analyzed. It was found that in the parameter regime where the network without heterogeneity would have been fully synchronized, an intermediate level of variability could segregate the network into two groups that burst alternately in time. On the other hand, stochastic neuroelectric noise caused cells to skip bursts; with enough noise a cell fired bursts only once in every two or more cycles of the population rhythm. At a high level of variability or noise the network became asynchronous.

In this paper we present an improved version of our RE network model. The single RE cell model is updated according to new voltage-clamp and current-clamp data (see METHODS). In contrast to our previous modeling, here the fast γ-aminobutyric acid-A ($GABA_A$) and slow $GABA_B$ synapses are treated separately, so that their different effects on the RE network behavior can be examined. The mathematical expressions for the model synaptic currents are compared quantitatively with experimental measurements. With this model we describe the different patterns that the RE network exhibits, determine their dependence on the model's parameter values, and assess the degree of network synchronization at different levels of variability and noise. Two possible synchronizing mechanisms intrinsic to the RE network are examined: $GABA_B$ synapses with a slow decay in the absence of $GABA_A$ inhibition and $GABA_A$ synapses with a reversal potential of -65 to -50 mV, less negative than usually assumed or estimated. In addition we study the effects of the TC cells on synchronization by considering a simple model of a single TC pool that acts as a source of coherent excitation to the RE network.

Preliminary results of this work have appeared in Golomb et al. (1993).

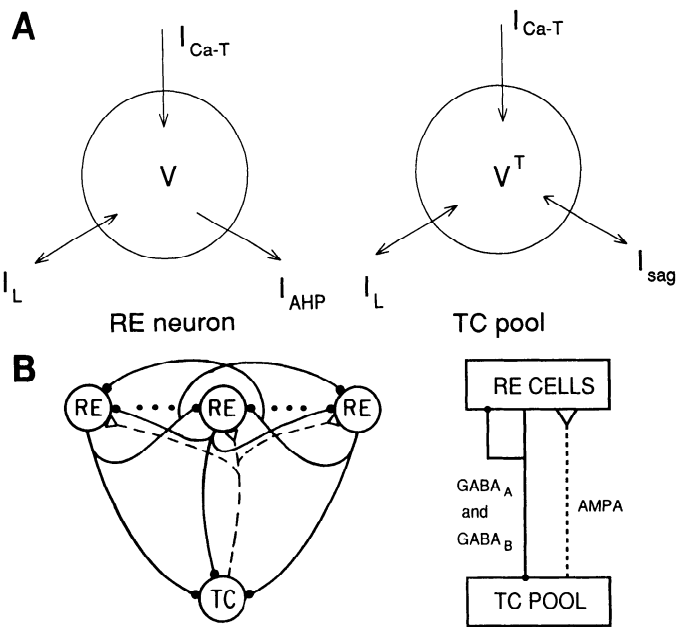

FIG. 1. Schematic diagram of our neuron model. The thalamic reticular (RE) cell has 3 intrinsic currents: a T-type calcium current $I_{Ca\text{-}T}$, a calcium-dependent potassium current I_{AHP}, and a leak current I_L. The thalamocortical (TC) pool also has 3 intrinsic currents: $I_{Ca\text{-}T}$, I_L, and a hyperpolarization-activated cation (sag) current I_{sag}. *B*: architecture of our network model. The RE cells are interconnected by γ-aminobutyric acid-A ($GABA_A$) and $GABA_B$ synapses. All the RE neurons inhibit the TC pool with $GABA_A$ and $GABA_B$ synapses and are excited by amino-3-hydroxy-5-methyl-4-isoxazolepropionic acid (AMPA) synapses from the TC pool.

METHODS

Single cell models

Each cell is represented by a single compartment according to the Hodgkin-Huxley-type scheme. Only the ionic currents that underlie the bursts are included. Currents for generating sodium spikes are not included for simplicity. The model's dynamic behavior is completely described in terms of differential equations, so stability analysis and bifurcation theory (Guckenheimer and Holmes 1983) can be used to analyze the system. In the following we present the differential equations that describe the two kinds of thalamic cells (Fig. 1*A*). The superscript RT denotes synaptic currents from the RE cells to the TC pool; no superscript is used for other synaptic currents. A cell's index (i) is also omitted here for simplicity.

RE CELL

$$C\frac{dV}{dt} = -I_{Ca\text{-}T} - I_{AHP} - I_L - I_{GABA\text{-}A} - I_{GABA\text{-}B} - I_{AMPA} \qquad (1)$$

The low-threshold calcium current $I_{Ca\text{-}T}$ causes rebound excitation on release from long-lasting hyperpolarization (McCormick and Huguenard 1992; Wang et al. 1991). The calcium-activated, voltage-independent potassium current I_{AHP} hyperpolarizes the cell after a burst. I_L is the leak current. The cell receives two kinds of inhibitory inputs: fast $GABA_A$ IPSPs and slow $GABA_B$ IPSPs. It also receives fast amino-3-hydroxy-5-methyl-4-isoxazolepropionic acid (AMPA)-mediated excitatory postsynaptic potentials from the TC pool. The state of the ith RE neuron, $i = 1, \ldots, N$, is characterized by seven state variables; one is the voltage and the others are gating variables for the intrinsic currents and synapses.

TC POOL

$$C\frac{dV}{dt} = -I_{Ca-T} - I_{sag} - I_L - I^{RT}_{GABA-A} - I^{RT}_{GABA-B} \quad (2)$$

The slow "sag" current I_{sag} (reversal potential −40 mV) is activated at hyperpolarized levels. The other currents are of the same types as in the RE cell, but they have different parameter values. The state of the TC pool is characterized by four state variables.

The intrinsic ionic currents are controlled by activation and inactivation variables. Such a generic variable x evolves in time according to the equation

$$\frac{dx}{dt} = [x_\infty(V) - x]/\tau_x(V), \quad (3)$$

where $\tau_x(V)$ is the time constant that may be voltage-dependent and $x_\infty(V)$ is the steady-state function of x, which has the form

$$x_\infty(V) = \{1 + \exp[-(V - \theta_x)/\sigma_x]\}^{-1} \quad (4)$$

The current I_{AHP} is exceptional because its gating variable depends on the intracellular calcium concentration and not on the membrane potential. The equations and the parameters of the model are given in the APPENDIX.

Network architecture

The RE network model consists of N globally (all-to-all) coupled neurons. We are interested in the limit of very large N. Self-coupling is included because it simplifies the analysis; it has a negligible effect when N is large. All the RE neurons are affected by the same global synaptic field. This field is produced by fast $GABA_A$ synapses, each with maximal conductance g_{GABA-A}/N, and slow $GABA_B$ synapses with maximal conductance g_{GABA-B}/N. With this scaling the maximal synaptic field is independent of N. Each RE cell inhibits the TC pool with $GABA_A$ and $GABA_B$ synapses with maximal conductances g^{RT}_{GABA-A}/N and g^{RT}_{GABA-B}/N, respectively. It is excited by the TC pool with maximal conductance g_{AMPA}. The model's architecture is shown schematically in Fig. 1*B*.

At the present time little quantitative data are available for the RE nucleus concerning the cell density and intrinsic connection patterns. Our rationale for using all-to-all coupling resides in the intuitive notion that this type of connectivity favors global synchronization, so an RE network with realistic wiring properties could not sustain a higher degree of synchrony than is found with all-to-all coupling. On the other hand, with their extensive dendritic arborizations (up to 1 mm in some directions; see Steriade et al. 1990), RE cells within a confined region are presumably strongly coupled, and our network model could be considered as reasonable for describing at least a sector of the RE nucleus a few millimeters in size.

Existence, stability, and basins of attractions

In principle, membrane potential time courses of neurons in the network are different for different initial conditions. Here we mostly limit ourselves to the network's behavior at long time, after transients have died away and it has converged to an attractor (Bergé et al. 1984). Simulations show that the system's time courses usually converge rapidly, i.e., within a few cycles, to time courses close to an attractor. Simple examples of attractors are resting states (fixed points) and periodic oscillations (limit cycles). For such a state to be an attractor it first has to it exist, i.e., to be a solution of the system of differential equations. In addition, it has to be stable, which means that small perturbations of the system's initial conditions near the solution will decay and the system will converge to it. For further explanation, see Bergé et al. (1984) and Guckenheimer and Holmes (1983).

There are parameter regimes in which our network exhibits multistability, i.e., more than one attractor exists. In such cases the system converges to one of the attractors depending on its initial conditions. When the initial conditions are chosen from a specific probability distribution we can define the relative volume of the stable state's basin of attraction (which is the set of initial conditions from which the system goes to the attractor) with respect to the probability distribution as follows. The relative volume is the fraction of trials in which the system converges to an attractor (or a set of attractors) when the initial conditions are chosen at random from this probability distribution. The relative volume depends on the probability distribution used (Golomb and Rinzel 1994b). However, by choosing a "reasonable" probability distribution we can learn about the relative importance of the attractors. In our simulations the initial condition for a cell's membrane potential was chosen at random from the interval (−70 mV, −50 mV). The other variables are initialized with their steady-state values corresponding to the chosen voltage.

Population-averaged variables and synchrony measure

The RE neural network is treated here as a large dynamic system. It is convenient to describe the properties of such a system by looking at population-averaged variables. An important population-averaged variable is the population-averaged voltage $V_{POP}(t)$, which corresponds to the "local field potential" of many RE neurons.

$$V_{POP}(t) = \frac{1}{N}\sum_{i=1}^{N} V_i(t) \quad (5)$$

A synchrony measure χ of the RE network is defined according to

$$\chi^2 = \frac{\lim_{T\to\infty}\frac{1}{T}\int_0^T dt(V_{POP}(t) - \bar{V}_{POP})^2}{\frac{1}{N}\sum_{i=1}^{N}\lim_{T\to\infty}\frac{1}{T}\int_0^T dt(V_i(t) - \bar{V}_i)^2} \quad (6)$$

where

$$\bar{V}_{POP} = \lim_{T\to\infty}\frac{1}{T}\int_0^T dtV_{POP}(t) \quad (7)$$

$$\bar{V}_i = \lim_{T\to\infty}\frac{1}{T}\int_0^T dtV_i(t) \quad (8)$$

This measure (Golomb and Rinzel 1993, 1994b) is the ratio between the time-averaged fluctuations of the population-averaged voltage V_{POP} and the population average over each cell's time-averaged V_i fluctuations. It is 1 when all the neurons have the same voltage time course and 0 for an incoherent state when the fluctuations of V_{POP} are zero. Numerically, these quantities are calculated over a sufficiently long time interval, after the system has converged to a stable state. Qualitatively, the system is highly synchronized if all the burst peaks shown in a rastergram (see RESULTS and *A* and *C* in Figs. 5–7 and 11) occur at about the same time relative to the oscillation period (for a quantitative measure see Pinsky 1993).

Modeling heterogeneity and noise

The real RE network is heterogeneous because parameters vary from cell to cell. Parameters that likely vary significantly include the maximal conductances of different ionic and synaptic currents, which relate to the total number of ionic channels per cell. In the limit of large N, random distributions of synaptic couplings (e.g., g_{GABA-A} and g_{GABA-B}) are averaged out in our case of global connectivity, and the important variabilities are those of the intrinsic ionic conductances. Because our main goal is to check the robustness of synchronized or partially synchronized solutions

to heterogeneity, we chose to introduce it into one parameter only, the maximal T-type calcium conductance g_{Ca} (Golomb and Rinzel 1993). This parameter is important because the cell is considered more "excitable" if it has a larger g_{Ca} value. For simplicity, the distribution of g_{Ca} is taken to be uniform with a mean $\bar{g}_{Ca}$ and a standard deviation σ_g. In reality, the distribution of g_{Ca} is expected to have a "tail" at large values. We expect that the tail neurons escape more easily from synchronization, but most of the other neurons behave similarly to what we predict with a uniform distribution. Heterogeneity in the synaptic time constants does not have a significant effect on the network dynamics.

In reality neurons are not deterministic. Synaptic transmission is a noisy process, and ion channel dynamics is also stochastic. Moreover, an important source of noise is the inputs from other brain centers, not included in the network. This factor affects only the membrane potential dynamics. It is modeled here as an additive noise $\xi_i(t)$ in the current balance equation, whereas the equations for the gating variables remain as before. The noise $\xi_i(t)$ is Gaussian, white, and uncorrelated (between neurons) with variance $2D$ (Van Kampen 1981).

The level of heterogeneity among cells is measured by the ratio $\sigma_g/\bar{g}_{Ca}$. One way to determine whether the noise level is high is by comparing the change of the membrane potential due to the deterministic versus stochastic terms in the neuron's current balance equation (*Eq. A1*). In hyperpolarized voltage regimes the membrane potential variation due to the deterministic terms (ionic currents) is ~10 mV. The stochastic noise variation of voltage fluctuations is $\sim(D\tau)^{1/2}$, where τ is a typical time constant. For example, if the voltage-dependent channels are ignored, τ is the membrane time constant $C/g_L = 17$ ms, and the stochastic contribution to the membrane potential change is ~4 mV if $D = 10^{-3}\text{V}^2/s$. Thus this noise level can be considered as "strong." Qualitatively, neuronal voltage time courses at hyperpolarized levels look "noisy" for $D \sim 10^{-3}\text{V}^2/s$ (see Figs. 6*C*, 7*C*, and 11*C*), but smooth at $D \sim 10^{-5}\text{V}^2/s$ (Fig. 5).

Computational and numerical methods

Most of this paper's results were obtained using numerical methods. The equations were integrated using the fourth-order Runge-Kutta method with time step $\Delta t = 0.5$ ms for noiseless equations and the Euler method with $\Delta t = 0.25$ ms for noisy equations. Simulations with smaller time steps confirmed the integration accuracy. We usually simulated the network with $N = 100$ and analyzed finite-size effects by using $N = 1{,}000$.

When the system segregates to one or more clusters (see RESULTS) it is convenient to investigate the dependence of the system's behavior on parameters by simulating only the reduced dynamics of the clusters themselves (Golomb and Rinzel 1994b; Golomb et al. 1992). The reduced equations of fully synchronized oscillations and cluster oscillations were integrated using the software package Dstool (Back et al. 1992). Stability analysis of homogeneous and cluster states was performed using the method developed by Golomb et al. (1992) and Golomb and Rinzel (1994b).

Strategy for dealing with many-parameter models

Even a highly idealized nonlinear model of a single neuron may display a great variety of response characteristics when a broad range of parameters is considered (Rinzel and Ermentrout 1989). Thus it is important to consider ranges of the biophysical parameters and to test different initial conditions. It is, of course, impossible to study the entire multidimensional space of parameters, especially when the investigation is based mostly on numerical simulations. We try to limit the range of parameters by taking most of their values from the literature. However, the variability between different experiments that evaluate a given parameter can sometimes be large. The maximal conductances of the intrinsic and the synaptic ionic currents are often hard to determine and are treated here as free parameters.

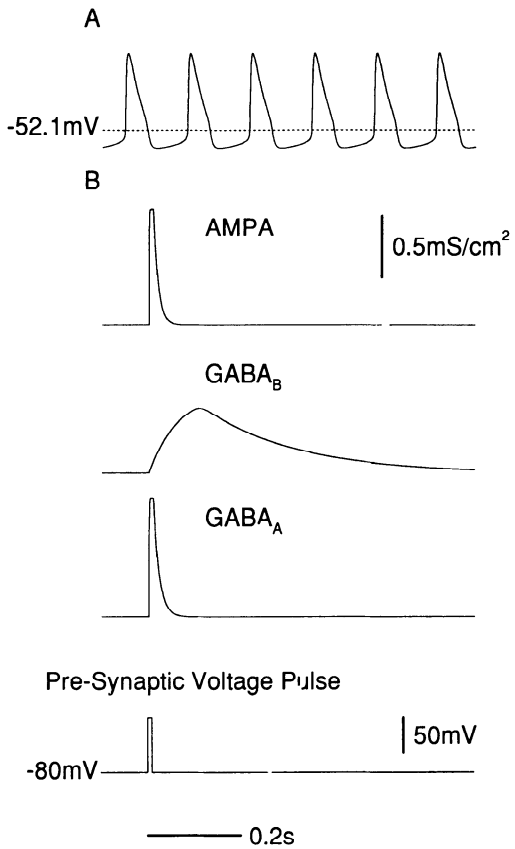

FIG. 2. Single cells and single synapses. *A*: single cell oscillates at 7.5 Hz with our reference parameters [AHP maximal conductance (g_{AHP}) = 0.3 mS/cm² (——)]. It is at rest with membrane potential −52.1 mV when I_{AHP} is blocked (· · ·). *B*: traces of synaptic conductances in response to a brief presynaptic voltage pulse of 10 ms. For this panel the maximal conductances are fixed at 1 mS/cm² for each synapse.

Knowing these difficulties we used the following strategy. We chose a biophysically plausible parameter set as a reference point in the parameter space (see APPENDIX). Starting from this point we vary one or two parameters at a time to study their effects. Exploring the dependence on parameters provides us with an understanding of the different dynamic patterns the network can exhibit. The details of the neuron dynamics, like the frequency and the amplitude of the cell's membrane potentials, are dependent on the specific parameters and thus comparison with experiments is only semiquantitative.

RESULTS

Single cells, synapses, and rhythmogenesis

A single RE cell in our model is a conditional oscillator. It either is at rest or it can oscillate, depending for example on the value of its leakage reversal potential (V_L). With our reference parameter set ($V_L = -60$ mV, see APPENDIX) it oscillates at 7.5 Hz (Fig. 2*A*); but when V_L is reduced to −80 mV it is at rest. Oscillations are generated by an adequately powerful T-type calcium conductance. A hyperpolarization mechanism is needed for deinactivating this conductance. At the single cell level this mechanism can be either due to a sufficiently negative V_L or due to an I_{AHP}. For example, blocking I_{AHP} abolishes the neural oscillations for $V_L = -60$ mV. However, if V_L is decreased to −80 mV,

the neuron becomes oscillatory again (at 3 Hz). The frequency is lower because the kinetics of the T-type calcium current at hyperpolarized voltages is slower. The I_{AHP} current is thus important to the behavior of the isolated cell, as a hyperpolarizing mechanism, to maintain endogenous oscillations in an appropriate frequency range.

In the RE network model, synaptic inputs can provide hyperpolarizing mechanisms. $GABA_B$ inhibition can hyperpolarize the cell, as can $GABA_A$ inhibition with a reversal potential that is negative enough (below −70 mV). The effects of I_{AHP} on the network behavior are minimal unless there is no other mechanism for providing hyperpolarization to the network (then, blockade of I_{AHP} abolishes network oscillations). Most of the network simulation results reported below would be little changed if I_{AHP} were absent. Because synaptic effects usually provide enough hyperpolarization for maintaining oscillations, questions about whether the single RE cell is an endogenous oscillator or not are mostly irrelevant to the network behavior.

Time courses of synaptic conductances after a brief presynaptic voltage pulse are shown in Fig. 2*B*. The $GABA_A$ and AMPA synaptic conductances decay rapidly after the pulse, whereas the $GABA_B$ synaptic conductance lasts for several hundred milliseconds (Otis et al. 1993).

Oscillation patterns in an isolated RE network

PATTERNS OF FULL, PARTIAL, AND NO SYNCHRONY. We start our investigation of the RE network with the simplest case of a homogeneous population without neuroelectric noise. Here we describe the possible states the system exhibits; their dependence on parameter values will be given below. Time courses of the membrane potentials of neurons in the RE network are shown in Fig. 3. Because neurons are identical, "uniform" behaviors exist (but may or may not be stable) in which all cells follow the same time course. Such a behavior may be a uniform resting state, in which all neurons have the same stationary membrane potential; a uniform periodic oscillation state, in which all cells oscillate together periodically (Fig.3, *E* and *F*); or (not often) a uniform aperiodic state. In addition, the system can be partially synchronized, because it segregates into clusters. A "cluster" denotes a group of neurons that behave in exactly the same way (i.e., have the same voltage time course); different clusters behave differently. In Fig. 3*A* there are two clusters; one is active and bursting and the other is almost quiescent. Other cluster states involve two or more active clusters. For instance, in Fig. 3*B* one of the two clusters of cells fires a sequence of three bursts, during which cells in the other cluster are inhibited at a hyperpolarized level. Then the second cluster takes over and emits five consecutive bursts while the first cluster remains inhibited. The process repeats itself periodically. In Fig. 3*C* there are three clusters, with a similar fraction of cells within each cluster. The three clusters oscillate ~120° out of phase. V_{POP} oscillates 3 times faster than every neuron (here 19 Hz compared with 6.3 Hz). Each time $V_{POP}(t)$ reaches a peak, about one third of the neurons burst, representing partial synchrony in the system. For different values of parameters and initial conditions the number of neurons in each cluster can be less uniform (Fig. 3*D*). In general, there can be cluster states with two, three, four or more clusters. Usually the number of clusters is small even for large N. However, in some cases there are several large clusters accompanied by several small ones [as found in models of globally coupled maps by Kaneko (1989, 1990)]. In most cases of clustering, but not always, the system oscillates periodically.

Note that in the active-quiescent cluster state as well as in the fully synchronized state the bursting rate of each active neuron is equal to the population rhythmic frequency. The quiescent neurons would not be detected in extracellular recordings (e.g., Buzsáki 1991; Fisher et al. 1992). If a microelectrode penetrates a quiescent cell (e.g., von Krosigk et al. 1993a) and a current pulse is injected, the cell may join the active cluster. In contrast, in the case of a network with two or more active clusters, each cell's frequency is only a fraction (1/2, 1/3, etc.) of the population rhythmic frequency.

The segregation of neurons into clusters depends on the system parameters as well as on the initial conditions. For a fixed parameter set the system can often exhibit cluster oscillations with different numbers of clusters. Even for a pattern with a fixed number of clusters, the number of neurons within each cluster can vary. There may be cluster states with the same number of clusters and the same numbers of neurons within each cluster, but with different voltage time courses. In addition, for a specific cluster state, the assignment of neurons to clusters depends on initial conditions, because cells are identical. Thus the system exhibits a large degree of multistability and displays an enormous number of patterns for the same parameters. A transition from fully synchronized oscillations to alternating cluster oscillations is often accompanied by an increase of the population frequency and a reduction of each cell's bursting rate.

The fully synchronized oscillations and the active-quiescent cluster states of the model may relate to biological behavior only if they are robust to heterogeneity and stochastic noise, in the sense that under such conditions the neurons' voltage time courses would remain similar to the homogeneous case. For fully synchronized oscillations the synchrony measure χ is 1, and when heterogeneity and noise are introduced, the system is considered as synchronous if χ remains ~1. The active-quiescent cluster states and states with two or more active clusters may have similar χ values. The measure χ is ~0 for asynchronous states where every neuron bursts independently, virtually unrelated to the bursting of the others. In an asynchronous state the averaged population quantities are almost constant in time, with fluctuations (as measured by χ) that decay like $N^{-1/2}$ when the number of cells N becomes large. (e.g., Abbott and Van Vreeswijk 1993; Golomb and Rinzel 1993, 1994a,b; Golomb et al. 1992; Hansel and Sompolinsky 1992; Kuramoto 1984).

PARTIAL SYNCHRONY (CLUSTERING) WITH HYPERPOLARIZING $GABA_A$ SYNAPSES. Starting with the homogeneous and noiseless network, we identify in Fig. 4 some parameter regimes (including the reference case with both $GABA_A$ and $GABA_B$ synaptic conductance) in which different stable patterns have been observed, i.e., obtained for our choice of random initial conditions. A filled bar represents a regime in which a pattern type has a sizeable basin of

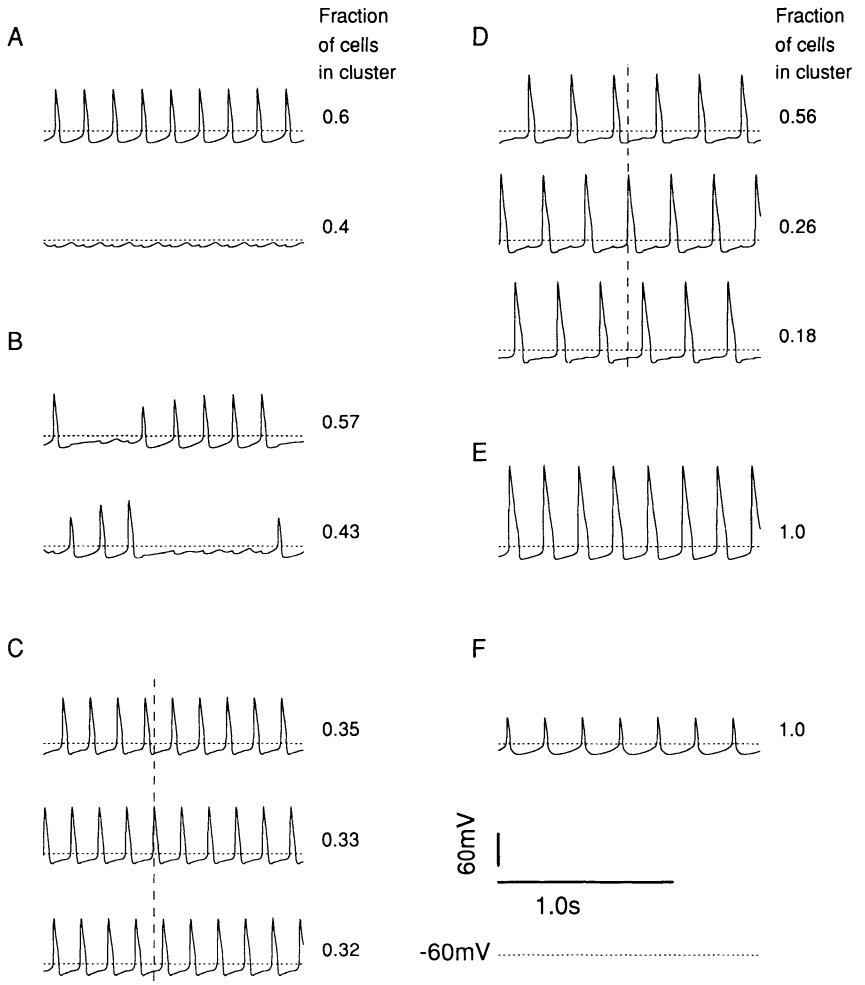

FIG. 3. Membrane potential time courses of neurons in an isolated RE network of identical cells (N = 100). Different parameter values yield periodic oscillations in which the neurons exhibit clusters or are fully synchronized. The fraction of cells in each cluster is specified alongside its trajectory. Parameters of the reference case (APPENDIX) are used [maximal T-type calcium conductance (g_{Ca}) = 2 mS/cm^2, maximal $GABA_A$ conductance ($g_{GABA\text{-}A}$) = 0.5 mS/cm^2, maximal $GABA_B$ conductance ($g_{GABA\text{-}B}$) = 0.1 mS/cm^2, and $GABA_A$ reversal potential $V_{GABA\text{-}A}$ = −75 mV] unless specified otherwise. The particular cluster patterns shown here co-exist with a huge number of other such patterns. Dotted horizontal line (in all figures): reference membrane potential of −60 mV. A: 1 cluster is active and bursts, whereas the other is almost quiescent and does not burst. This pattern coexists with a 2-cluster pattern in which clusters alternately fire a sequence of 5 and 3 bursts (B). C: blockade of $GABA_B$ synapses ($g_{GABA\text{-}B}$ = 0) leads to 3 clusters that have about the same number of neurons and that oscillate at ~120° out of phase. The population voltage V_{POP} oscillates at high frequency (~19 Hz). D: with g_{Ca} = 3.5 mS/cm^2 instead of 2.0 mS/cm^2, another 3-cluster state is observed, with a different fraction of neurons in each cluster. E: with g_{Ca} = 3.5 mS/cm^2 and $GABA_A$ synapses blocked ($g_{GABA\text{-}A}$ = 0) the network oscillates periodically and uniformly. F: with $V_{GABA\text{-}A}$ = −60 mV instead of −75 mV, the network oscillates periodically and uniformly.

attraction for our choice of initial conditions (see METHODS). An open bar represents a regime in which this pattern type is stable, but the relative volume of its basin of attraction is negligible. We calculated the borders of these regimes only for the uniform states.

With low values of g_{Ca} (Fig. 4, A and B), the system is not excitable enough and is stable at rest; maintained oscillations were not found. As g_{Ca} is increased the network starts to oscillate, but in general not in full synchrony. Instead the system exhibits cluster oscillations, either with one active cluster or with two or more active clusters. In some parameter regimes the fully synchronized oscillation is not a stable pattern of the system. In other parameter regimes full synchrony is stable, but the system prefers to segregate into clusters because these patterns attract most of the initial conditions. In many parameter regimes the system shows multistability, because several types of patterns were actually observed for different initial conditions taken from the same distribution (see METHODS).

With our reference parameter set (see APPENDIX), the homogeneous network displays active-quiescent cluster oscillations (Fig. 3A). Various oscillatory patterns with multiple-bursting active clusters are also obtained for different initial conditions (e.g., see Fig. 3B). Figure 5 shows the effects of heterogeneity (A and B) or noise (C and D) for this parameter set. The synchrony measure χ drops as the level of heterogeneity is increased, very abruptly for low heterogeneity levels and then more gradually (Fig. 5B). As $\sigma_g/\bar{g}_{Ca}$ exceeds 0.25, χ falls to a level of ~0, corresponding with asynchronous behavior. Rastergrams and traces of the population voltage $V_{POP}(t)$ are shown in Fig. 5A for $\sigma_g/\bar{g}_{Ca}$ = 0.05. At this heterogeneity level, neurons with low g_{Ca} values are quiescent, whereas those with higher g_{Ca} values are bursting. V_{POP} has a strong periodic component, even though it is not strictly periodic. The neurons tend to burst in synchrony with the population voltage, but most active cells burst at every second or third cycle. Thus, as for cluster states with two or more active clusters, a neuron's bursting rate is a fraction of the global frequency, although not necessarily a simple fraction like 1/2 or 1/3. In this particular example, although most active neurons burst at half of the network frequency, they do not segregate into two well-defined groups. In a sense, neurons jump from group to group. For somewhat different parameters (e.g., GABA-A reversal potential ($V_{GABA\text{-}A}$) = −72 mV and $\sigma_g/\bar{g}_{Ca}$ = 0.02) the neurons do segregate into two groups bursting alternately based on their g_{Ca} values (see also Golomb and Rinzel 1993).

A miniscule amount of stochastic noise precludes the active-quiescent cluster state. Even for $0 < D < 10^{-5}$ V$^2/s$, the active-quiescent clusters are destroyed, and χ drops from 0.7 to 0.5 (Fig. 5D). For $D = 10^{-5}$ V$^2/s$, V_{POP} has a strong periodic component (Fig. 5C). A typical neuron's voltage time course (V_1) fluctuates with the same fre-

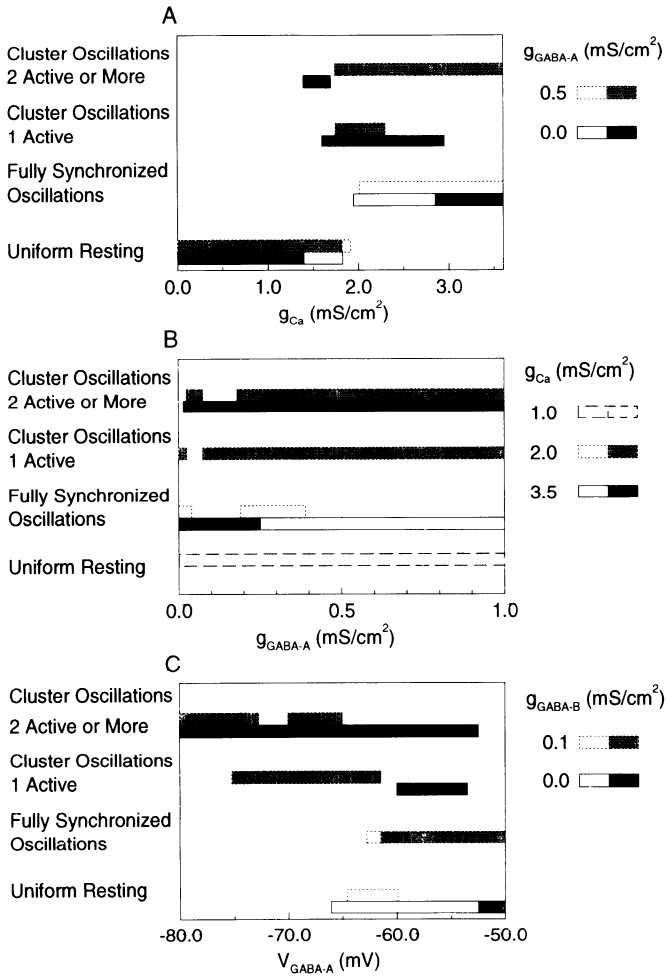

FIG. 4. Existence and basins of attraction sizes for different stable behavior states as functions of parameters. States associated with open bars attract a small fraction of randomly chosen initial conditions. In the filled bars, patterns have a large attraction basin. The existence and stability of these patterns are determined by an independent method (see METHODS). To estimate their attraction basins, simulations were performed with 10 different sets of initial conditions. If an attractor had been obtained at least once, its basin of attraction is assumed to be large. Otherwise it is assumed to have a small basin of attraction. The fully synchronized oscillations are periodic in time. The network states are divided into 4 categories: uniform resting, fully synchronized oscillations (Fig. 3, *E* and *F*), cluster oscillations with only 1 active cluster (Fig. 3*A*), and cluster oscillations with ≥2 active clusters (Fig. 3, *B–D*). *A*: dependence on g_{Ca} for g_{GABA-A} = 0.5 mS/cm^2 (- - -, gray bar) and g_{GABA-A} = 0 (——, black bar). At low g_{Ca} values the system is at rest. At higher g_{Ca} values (>2.0 mS/cm^2) it oscillates, generally not in synchrony. Fully synchronized oscillations are obtained for large g_{Ca} and low g_{GABA-A} values. *B*: dependence on g_{GABA-A} for g_{Ca} = 1 mS/cm^2 (— — —, light gray bar), 2 mS/cm^2 (- - -, dark gray bar), and 3.5 mS/cm^2 (——, black bar). *C*: dependence on V_{GABA-A} for g_{GABA-B} = 0.1 mS/cm^2 (- - -, gray bar) and g_{GABA-B} = 0 (——, black bar). With hyperpolarizing inhibition (i.e., sufficiently negative V_{GABA-A} values) the system does not oscillate in synchrony. Active-quiescent states are found for intermediate V_{GABA-A} values, usually in coexistence with states having ≥2 active clusters. With shunting $GABA_A$ inhibition (V_{GABA-A} > −61.5 mV) and g_{GABA-B} = 0.1 mS/cm^2, the network oscillates uniformly and periodically. When g_{GABA-B} is blocked, RE cells do not fire rebound bursts if V_{GABA-A} is not negative enough to supply the needed hyperpolarization, and the network is at rest.

quency as V_{POP}, but bursts only once in every few cycles. The smoothness of this time course indicates a low noise level. This behavior is similar to that observed in a simpler model of RE neurons with noise (Golomb and Rinzel 1994b). Gradual decrease of χ with $D > 10^{-5}$ V$^2/s$ leads to the reduction in amplitude of the global population oscillations. The system bursts asynchronously for $D > 3 \times 10^{-4}$ V$^2/s$ (not shown).

FULL SYNCHRONY WITHOUT $GABA_A$ SYNAPSES. Despite the fact that the fully synchronized oscillations exist for large enough g_{Ca} values (Fig. 4, *A* and *B*), they are actually observed only when $GABA_A$ IPSPs are sufficiently weak (see

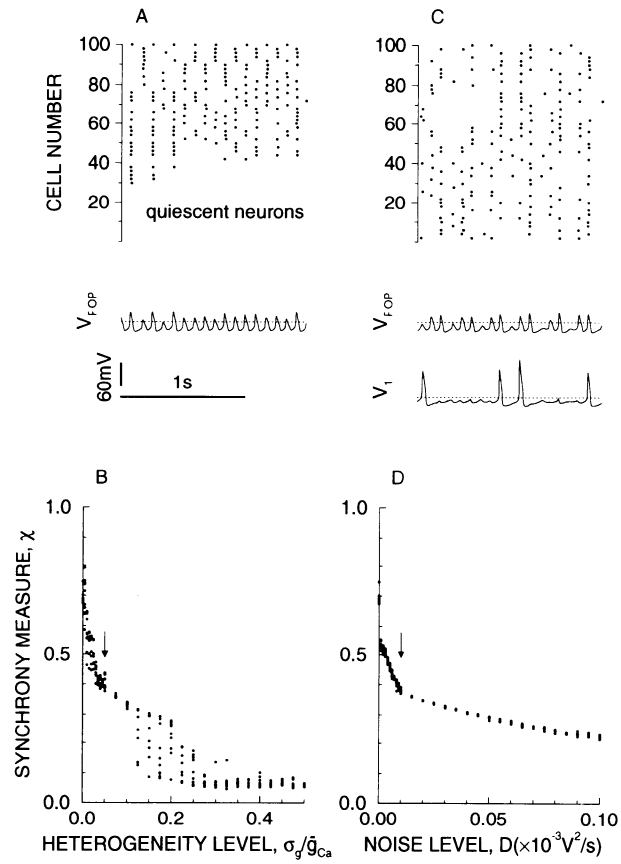

FIG. 5. Effects of heterogeneity (*A* and *B*) and noise (*C* and *D*) on the oscillatory dynamics of an isolated RE network. The reference parameter set is used (see APPENDIX and Fig. 3, *A* and *B*). The rastergrams (*A* and *C*) show burst times of every other simulated neuron (50 of the total 100 cells). The neurons are ordered according to their g_{Ca} values in *A* (*neuron 100* with the highest g_{Ca}) and randomly in *C*. The burst times correspond to the membrane potential peaks that exceed −45 mV, the assumed threshold for sodium spiking. The particular cases *A* and *C* correspond to heterogeneity ($\sigma_g/\bar{g}_{Ca}$ = 0.05) and noise ($D = 10^{-5}$ V$^2/s$) marked by the arrows in *B* and *D*, respectively. V_{POP} is plotted below the rastergram. *C*: time course (V_1) of a single neuron is also plotted. Dotted horizontal line: reference voltage level of −60 mV. The synchrony measure χ (see METHODS) is plotted vs. heterogeneity in *B* and vs. noise in *D*. For each value of heterogeneity or noise the system was simulated with 10 sets of different initial conditions for 15 s and the χ values were calculated using *Eq. 6* by averaging over the last 10 s. At 0 heterogeneity and noise the system exhibits either an active-quiescent cluster state (Fig. 3*A*) or a 2-cluster state with alternating multiple bursting (Fig. 3*B*). *B*: synchrony measure decreases abruptly with heterogeneity <0.05. At small but finite heterogeneity levels neurons with large g_{Ca} values burst in synchrony with the population voltage, but only once in every ≥2 cycles. Neurons with small g_{Ca} values do not burst (*A*). At high heterogeneity levels (>0.25) the system behaves asynchronously; V_{POP} (not shown) is nearly constant. The χ values are not 0 because the number of cells *N* is finite. *D*: very small noise level reduces χ sharply from 0.75 to 0.55 (very near the ordinate). All the neurons burst together with V_{POP}, but not at every period (*C*). At high noise levels ($D > 3 \times 10^{-4}$ V$^2/s$, not shown) the system is asynchronous.

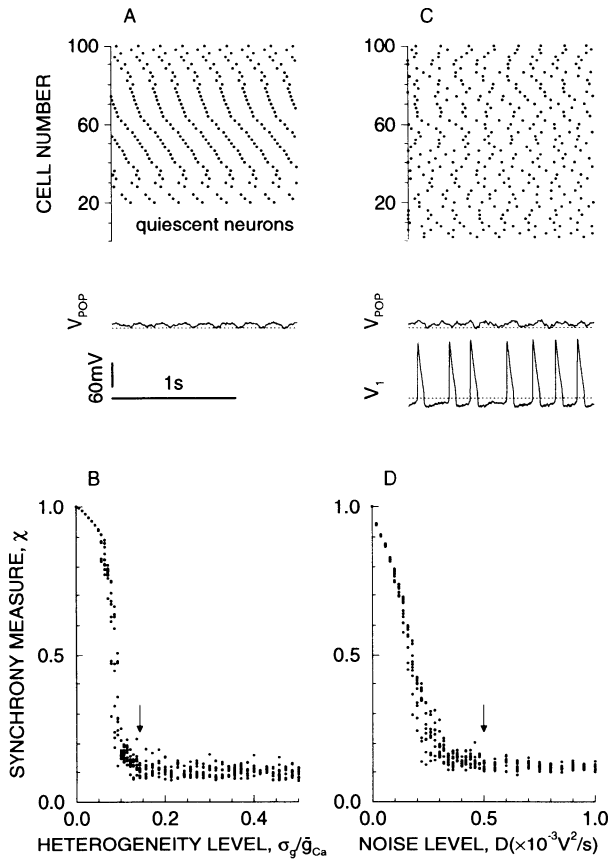

FIG. 6. Effects of heterogeneity (A and B) and noise (C and D) on the dynamics of the RE network dominated by the slow $GABA_B$ inhibition (with $GABA_A$ blocked and $g_{Ca} = 3.5$ mS/cm^2). Panel format as in Fig. 5. The rastergrams (A and C) correspond with heterogeneity ($\sigma_g/\bar{g}_{Ca} = 0.14$) and noise ($D = 5 \times 10^{-4}$ V^2/s) marked by the arrows in B and D, respectively. At 0 heterogeneity and noise the system oscillates periodically and uniformly (Fig. 3E). It tolerates small levels of heterogeneity (B), but at higher levels it goes to the asynchronous state (as shown in A) with V_{POP} almost constant in time. Neurons with small g_{Ca} values are quiescent; those with larger g_{Ca} values burst periodically, their bursting rates being an increasing function of g_{Ca} values. Low noise level maintains high synchrony (D), whereas at high noise levels the system is asynchronous; all the neurons burst but in random phases with each other, and V_{POP} is almost constant (C).

Fig. 3E). At very low $GABA_A$ levels they are the unique pattern, whereas at a higher level they coexist with cluster states having two or more active clusters.

We studied the effects of heterogeneity and noise on the synchronized state while blocking $GABA_A$ ($g_{GABA\text{-}A} = 0$) and with $g_{Ca} = 3.5$ mS/cm^2. The results are shown in Fig. 6. At low levels of heterogeneity the system is still highly synchronized. At a moderate heterogeneity level synchrony decreases sharply and the system goes to the asynchronous state (Fig. 6B). An example of the asynchronous state is given in Fig. 6A. In this case, macroscopic quantities, like V_{POP} and the averaged $GABA_B$ synaptic fields, are almost constant in time. Thus each neuron is affected by constant $GABA_B$ inhibition. It bursts periodically if its g_{Ca} value is large enough; otherwise it is at rest. Note that the rastergram looks ordered, but the bursting frequency of individual neurons varies weakly with their g_{Ca} values, from 5.59 to 5.15 Hz. Neurons with similar g_{Ca} values have similar frequencies and become dephased only after a long time.

Increasing the level of stochastic noise reduces gradually the synchrony measure χ until the system reaches an asynchronous state (Fig. 6D). In this state the neurons burst asynchronously (Fig. 6C) and the population voltage is again almost constant in time (Golomb and Rinzel 1994b).

FULL SYNCHRONY WITH SHUNTING $GABA_A$ SYNAPSES. Until now we have assumed that the $GABA_A$ synapses are inhibitory with a reversal potential of $V_{GABA\text{-}A} = -75$ mV (Bal and McCormick 1993). Although this reversal potential is difficult to determine accurately in RE neurons (see reference 13 in von Krosigk et al. 1993a), there are experimental indications that it may be less negative (J. Huguenard, private communication; Spreafico et al. 1988). On the other hand, $GABA_B$ IPSPs among RE neurons have not been demonstrated up to date. Therefore we studied the dependence of the network behavior on $V_{GABA\text{-}A}$, with or without $GABA_B$ synapses (Fig. 4C). In the presence of $GABA_B$ IPSPs the network displays both of the two types of cluster oscillations if $V_{GABA\text{-}A}$ is sufficiently negative. As $V_{GABA\text{-}A}$ is increased (just above -65 mV) the only observed oscillation type is the active-quiescent cluster state; this gives way to full synchronization for $V_{GABA\text{-}A} > -61.5$ mV (Fig. 3F). The fully synchronized oscillations are lost if $GABA_B$ is completely blocked. In that case, either cluster oscillations or the resting state are obtained.

For $V_{GABA\text{-}A} = -64$ mV the active-quiescent cluster states persist as heterogeneity is introduced; the population divides into two groups, one oscillating periodically with high synchrony and the other almost quiescent. Neurons with high g_{Ca} values burst at the same frequency ($\sim$7 Hz) as the population rhythm (Fig. 7A), whereas those with low g_{Ca} values do not burst at all and fluctuate weakly around -66 mV (similar to the quiescent neurons in the homogeneous case). However, in contrast with the previous cases (Fig. 5A; Golomb and Rinzel 1993), here the bursting rate is not a monotonic function of g_{Ca}, because neurons with intermediate g_{Ca} values might be totally quiescent or burst at every cycle, depending on the initial conditions. This phenomenon was confirmed in larger networks with N = 1,000. As heterogeneity is increased more neurons are recruited into the active group, and thus we observe the counterintuitive phenomenon that the synchrony measure χ, averaged over initial conditions, increases with the heterogeneity level σg (Fig. 7B).

The effect of noise is even more dramatic. Low noise levels destroy the active-quiescent cluster state. All the neurons fire in high synchrony with the population voltage, but from time to time a neuron skips a burst (Fig. 7C). Note that the noise level in this example is large, as demonstrated by the fluctuations of neuronal voltage V_1. As the noise level increases from low levels, χ increase rapidly; the active-quiescent cluster state is replaced by highly synchronized bursting (Fig. 7D). As the noise level is further increased, the degree of synchrony, as measured by χ, decreases as expected but gradually. With both heterogeneity and noise (e.g., $\sigma_g = 0.5$, $D = 0.5$) the network still displays rhythmic bursting with a high degree of coherence. In that case the bursting rate is a monotonic increasing function of g_{Ca} values.

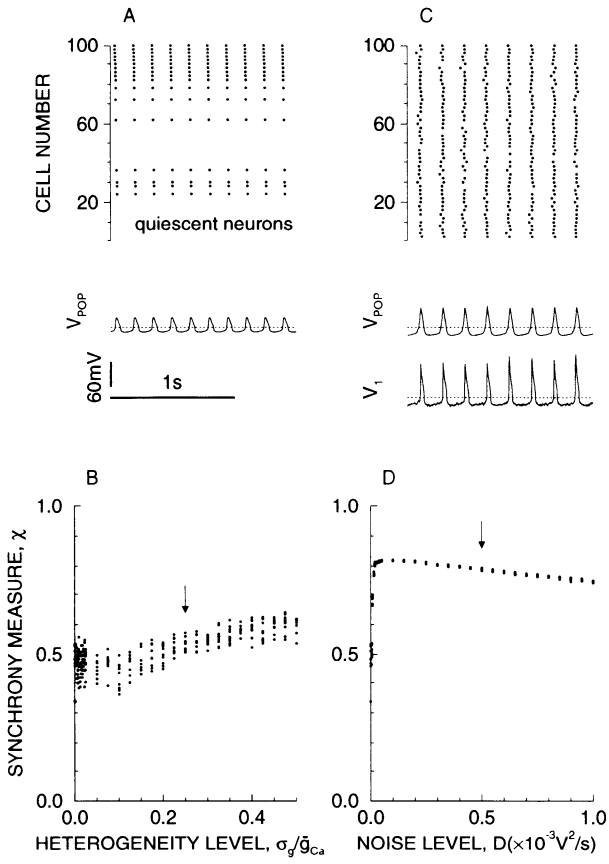

FIG. 7. Effects of heterogeneity (*A* and *B*) and noise (*C* and *D*) on the network dynamics of the RE network with shunting $GABA_A$ inhibition ($V_{GABA\text{-}A} = -64$ mV). Panel format as in Fig. 5. The rastergrams (*A* and *C*) correspond with heterogeneity ($\sigma_g/\bar{g}_{Ca} = 0.25$) and noise ($D = 5 \times 10^{-4}$ V^2/*s*) marked by the arrows in *B* and *D*, respectively. At 0 heterogeneity and noise the system exhibits an active-quiescent cluster state. The segregation into active and quiescent groups persists also in the heterogeneous network. Neurons with large g_{Ca} values burst in synchrony with the population voltage (*A*); neurons with small g_{Ca} values fluctuate weakly around a rest state of approximately −66 mV; Neurons with intermediate g_{Ca} values either burst or are silent. As the level of heterogeneity increases, more neurons on average become active, and thus χ increases slightly (*B*). Low noise level breaks the structure of active-quiescent clusters, and all the neurons burst in synchrony with V_{POP} (*C* and *D*). As the noise level increases further, χ decreases because the burst timings become less in phase with V_{POP}.

For $V_{GABA\text{-}A} = -60$ mV the homogeneous and noiseless network is in full synchrony. Heterogeneity and noise reduce the synchronization level only slightly but monotonically over the same ranges as in Fig. 5, *B* and *D*. For example, $\chi = 0.8$ at $\sigma_g/\bar{g}_{Ca} = 0.5$ and $\chi = 0.85$ at $D = 10^{-3}$ V^2/*s*.

PARTIAL CONNECTIVITY EFFECTS WITH A SMALL NUMBER OF NEURONS. We have studied the RE model for an all-to-all architecture. However, the results apply also to the case of partial connectivity when *1*) the probability that a neuron is postsynaptic to another is f and *2*) the average number fN of synaptic inputs to a neuron is large. In this case we scale the maximal $GABA_A$ and $GABA_B$ conductances as $g_{GABA\text{-}A}/fN$ and $g_{GABA\text{-}B}/fN$, respectively, to minimize the synaptic field's dependence on f and N. Using the methods described in Golomb and Rinzel (1994b) one can show under these conditions that the uniform resting state and the fully synchronized oscillations and cluster oscillations have the same existence and stability properties as in the all-to-all case. The intuitive reason is clear: in these states each neuron receives on average the same synaptic field as in the all-to-all case, whereas fluctuations from the average scale like $\sqrt{(1-f)/(fN)}$ and are negligible at large fN. Heterogeneity in the maximal synaptic conductance has similar effects as partial connectivity.

When N is not large enough fluctuations may be important and may reduce the degree of synchrony. These "finite-size effects" are stronger when N or f is smaller and for fixed N and f they depend on the other parameter values. We have found here that when a synchronized or a partially synchronized pattern is more robust to heterogeneity and noise it is also more robust to finite-size effects with partial connectivity. The fully synchronized state obtained with shunting inhibition (with the $GABA_A$ reversal potential around −60 mV, see Fig. 3*F*) is not sensitive to partial connectivity. Even for $f = 0.1$ the synchrony measure χ reduces only modestly, on average to 0.92 for $N = 1{,}000$ and to 0.84 for $N = 100$, and the membrane potential time courses are essentially the same as for $f = 1$. The fully synchronized state obtained with slow $GABA_B$ inhibition (with the $GABA_A$ synapses totally blocked and $g_{Ca} = 3.5$ mS/cm^2, see Fig. 3*E*) is less robust at small N and f. For $f = 0.5$, χ reduces to 0.90 for $N = 1{,}000$ but to 0.14 for $N = 100$. In the first case the behavior is similar to the all-to-all situation; in the latter case only little synchrony remains and the neurons burst almost randomly in time.

We checked partial connectivity effects also for our reference parameter set (cluster states with all-to-all coupling, see Fig. 3, *A* and *B*). With $f = 0.5$ and $N = 1{,}000$ or $N = 100$ the population voltage is nearly periodic, and cells burst once in every two or more cycles; also, some cells are quiescent. The system is sensitive to partial connectivity effects when N is small, just as it is sensitive to heterogeneity and noise.

Oscillation patterns in an RE-TC network

AMPA EXCITATION SYNCHRONIZES THE RE NETWORK. Adding the TC pool into the network increases significantly the number of parameters that the network's behavior depends on. However, a general result was obtained for all of the parameters we have tried: the TC pool tends to synchronize the RE network. A typical case is shown in Fig. 8 for a network of identical RE neurons with our reference parameter set. Without the TC pool the system exhibits cluster oscillations, either with one active cluster or two or more active clusters. A modest amount of excitation from the TC pool causes the RE network to burst in full synchrony (Fig. 8). The TC pool is also well synchronized with the RE network. A careful examination reveals that the TC pool starts to burst a short time (~1 ms) before the RE cells, determining the bursting frequency of the whole network.

We studied the effects of changing the g_{Ca} of the RE cells and the g_{AMPA}. In Fig. 9 are shown regions of the (g_{Ca}, g_{AMPA})-parameter plane where different stable network behaviors exist (regardless of their basins of attraction). The fully synchronized periodic oscillations are attractors in the gray regime, where g_{Ca} is high enough or g_{AMPA} is strong enough. The resting state is stable for $g_{Ca} \leq 2$ mS/cm^2,

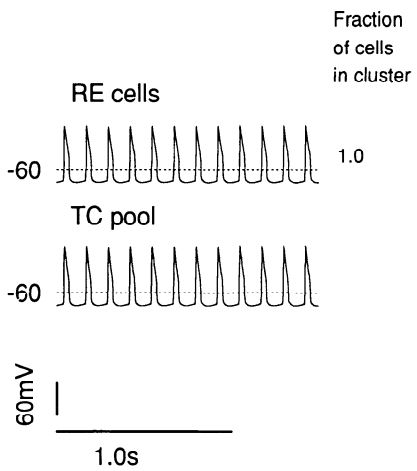

FIG. 8. RE network in reciprocal interaction with a TC pool. Membrane potential time courses of the RE neurons and the TC pool were obtained from a simulation with $N = 100$ and the reference parameters (AMPA maximal conductance $g_{AMPA} = 0.1$ mS/cm^2). The RE network is fully synchronized. The TC pool is phased-locked to the RE cells, but it starts bursting a short time earlier ($\sim$1 ms), pacing the oscillation frequency.

almost independently of g_{AMPA}. As representative of a cluster state, we calculated the borders of the regime in which a two-cluster state (50% of neurons in each cluster) is stable, without discriminating between states showing one active cluster and states showing two or more active clusters. The regime is limited to low g_{AMPA} values ($g_{AMPA} < 0.05$ mS/cm^2).

The patterns that are actually observed for our choice of random initial conditions are identified in Fig. 10. Although cluster states are observed at low AMPA, a modest AMPA excitation eliminates them in favor of the uniform oscillations. At low g_{Ca} values the system is still at rest with modest g_{AMPA} values, despite the fact that the uniform oscillations are stable patterns (Fig. 9). AMPA excitation of large coupling strength can create synchronous oscillations for small g_{Ca} values that coexist with the rest state. At even larger values of g_{AMPA} (>0.7 mS/cm^2 for $g_{Ca} = 1$ mS/cm^2) these oscillations become the only stable pattern (not shown).

The synchronous oscillation state induced by AMPA synapses is robust to heterogeneity and noise. As shown in Fig. 11, the synchronization measure χ is reduced only slightly even for $\sigma_g/\bar{g}_{Ca} = 0.5$ (Fig. 11*B*) or $D = 10^{-3}$ V^2/*s* (Fig. 11*D*), and the rastergrams exhibit a high degree of synchronization (Fig. 11, *A* and *C*). Partial connectivity among RE cells does not have anysignificant effect on the system dynamics.

DEPENDENCE OF FREQUENCY ON SYNAPTIC COUPLING. We have shown that, with fast excitation of TC origin, the RE network oscillates in synchrony. The oscillation frequency depends on the strength of the TC-RE reciprocal coupling. The magnitude of AMPA excitation has almost no effect on frequency, as long as it is strong enough to produce coherent oscillations. Under this condition the frequency dependence on $GABA_A$ and $GABA_B$ coupling among the RE neurons is also weak. On the other hand, the frequency is sensitive to blockade or enhancement of the inhibition from RE neurons to the TC pool. In Fig. 12 the burst frequency is plotted versus the coupling strength of $GABA_A$ (*A*) or $GABA_B$ (*B*) IPSPs. The frequency increases with the $GABA_A$ level and decreases with the $GABA_B$ level.

In the network the TC pool determines the frequency by bursting slightly before the RE cells. The frequency's decrease with $GABA_B$ is expected. More inhibition causes the TC pool to spend more time at hyperpolarized voltages, where the kinetics of the T-current is slow. At a first sight it

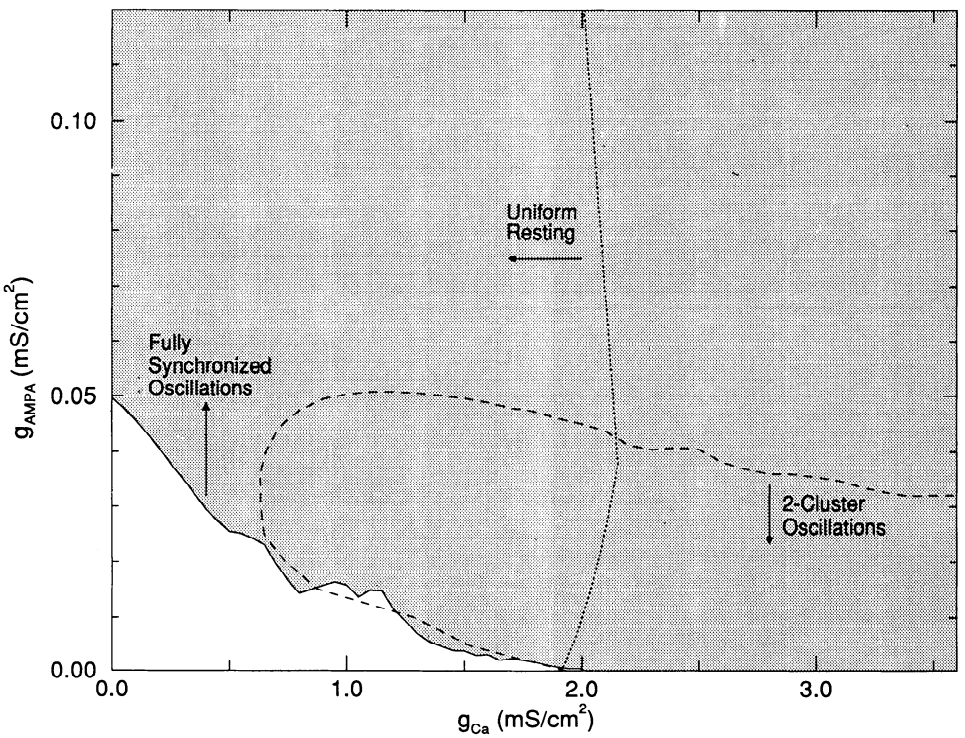

FIG. 9. Regimes in which different patterns exist and are stable are described in a 2-parameter phase diagram (g_{Ca} and g_{AMPA} of RE cells) for an RE-TC network with identical RE neurons. Basins of attraction are not considered. Fully synchronized periodic oscillations are stable in the grey regime. The uniform resting state is stable to the *left* of the dotted curve. We found stable 2-cluster states (of all types) with 50% of neurons in each cluster in the "thumb" region bounded by the dashed line. No such cluster states were found outside this region. No discrimination is made in this figure between active-quiescent states and states with 2 active clusters. However, it is clear that the 2-cluster state with equal number of neurons is limited to small g_{AMPA} values. Simulations show that all cluster states are limited to small g_{AMPA} (see Fig. 10); for modest or high g_{AMPA} values the network is uniform (fully synchronous).

seems surprising that increasing the strength of $GABA_A$ inhibition increases the frequency. One reason is that when $GABA_A$ inhibition from the RE cells is enhanced the TC pool bursts are quickly cut off by $GABA_A$ IPSPs, they become shorter, and the neuron is reset faster to a hyperpolarized level; as a consequence, the time period decreases. Another underlying mechanism is related to the kinetics of the TC pool's sag current. During a cycle's hyperpolarizing phase the sag current activates slowly, whereas during the depolarizing phase (the burst) the sag current inactivates rapidly. How long the hyperpolarizing phase must last depends on the amount of inward sag current needed to give rise to a rebound burst in the TC pool. During a shortened burst the sag current has less time to inactivate, so its average level remains higher. Consequently, during the next hyperpolarizing phase after a burst, the sag current requires less time to reach adequate activation for eliciting another rebound burst. Thus faster rhythm results. When the sag current is blocked the effect is strongly reduced but still exists because of the first mechanism (Fig. 12).

DISCUSSION

The isolated RE network model exhibits many modes of dynamic behavior. We emphasize qualitative trends in the dependence of these behaviors on parameters (which can be compared with experimental results) but realize that their quantitative features may change with other parameters that are kept constant. Still, from our computational results of this model and from those of simpler models studied previously (see INTRODUCTION), we draw several conclusions that are generic and that are not dependent on the specific parameter values. First, the postinhibitory rebound response generated by the T-current is crucial for the neural oscillations (Steriade et al. 1990). Second, there should be a mechanism for hyperpolarizing the RE cell to deinactivate the T-current. This can be achieved by a sufficiently negative leak reversal potential, by I_{AHP}, by $GABA_B$ inhibition, or by $GABA_A$ inhibition with a sufficiently negative reversal potential. Third, clustering behavior (partial synchrony, here mediated mainly by $GABA_A$) is found in many parameter regimes. The isolated RE network especially tends to show clustering patterns (including states with multiple bursts), as the parameters vary. Fourth, two mechanisms can robustly synchronize an inhibitory network. One way is with inhibition dominated by slow $GABA_B$ with only weak hyperpolarizing $GABA_A$. In addition, we discovered here that shunting $GABA_A$ inhibition can robustly synchronize the network. Fifth, by extending the model to include the TC pool, we have shown the synchronizing effect of AMPA excitation on the RE cells and the possibility of rhythmo-

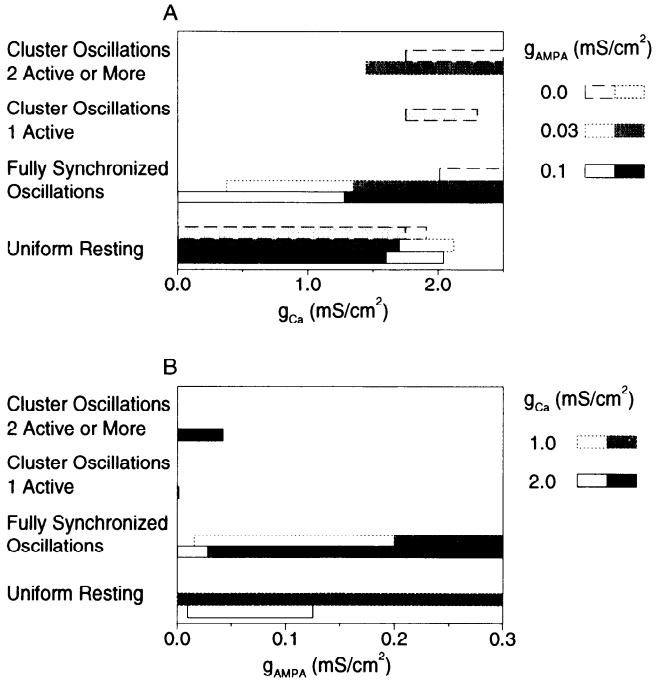

FIG. 10. Parameter regimes for behavioral states that are stable and have sizeable basins of attraction for the RE-TC network. Panel format as in Fig. 4. *A*: dependence on g_{Ca} for $g_{AMPA} = 0$ (— — —, light gray bar), $g_{AMPA} = 0.03$ mS/cm^2 (- - -, dark gray bar), and $g_{AMPA} = 0.1$ mS/cm^2 (——, black bar). For low g_{Ca} values the system is at rest. Without AMPA excitation, cluster oscillations are found for higher g_{Ca} values. At $g_{AMPA} = 0.03$ mS/cm^2, fully synchronized periodic oscillations coexist with states having ≥2 active clusters. At $g_{AMPA} = 0.1$ mS/cm^2 the system bursts periodically and uniformly for sufficiently large g_{Ca} values. *B*: dependence on g_{AMPA} for $g_{Ca} = 1$ mS/cm^2 (- - -, gray bar) and $g_{Ca} = 2$ mS/cm^2 (——, black bar). A sufficiently strong AMPA excitation can produce oscillations in a regime where without excitation the RE network is at rest.

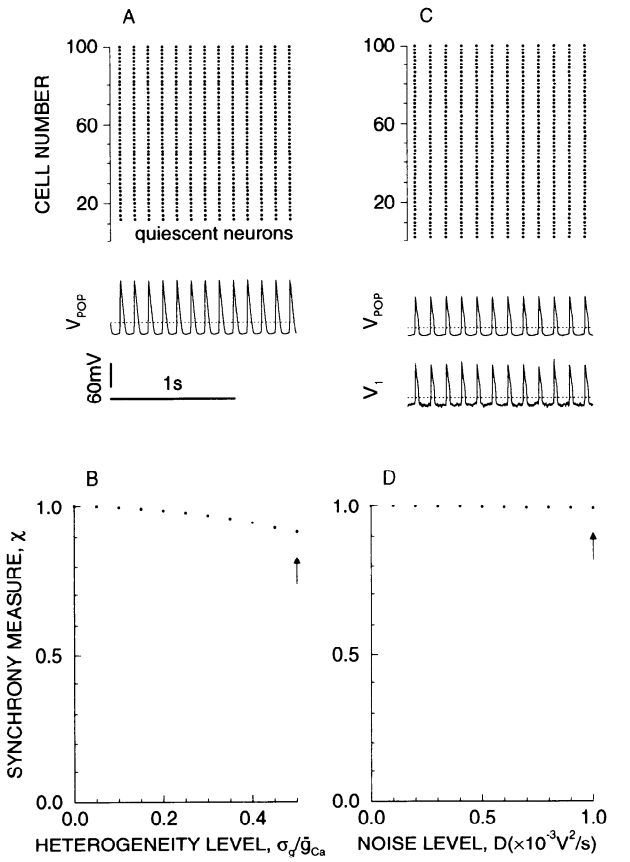

FIG. 11. Effects of heterogeneity (*A* and *B*) and noise (*C* and *D*) in RE neurons on the RE-TC network dynamics (with $g_{AMPA} = 0.1$ mS/cm^2). Panel format as in Fig. 5. The rastergrams (*A* and *C*) correspond with heterogeneity ($\sigma_g/\bar{g}_{Ca} = 0.5$) and noise ($D = 10^{-3}$ V^2/*s*) marked by the arrows in *B* and *D*, respectively. At 0 heterogeneity and noise the RE neurons oscillate periodically and uniformly (Fig. 8). A high degree of synchronization is maintained even with high levels of heterogeneity (*A* and *B*) and noise (*C* and *D*).

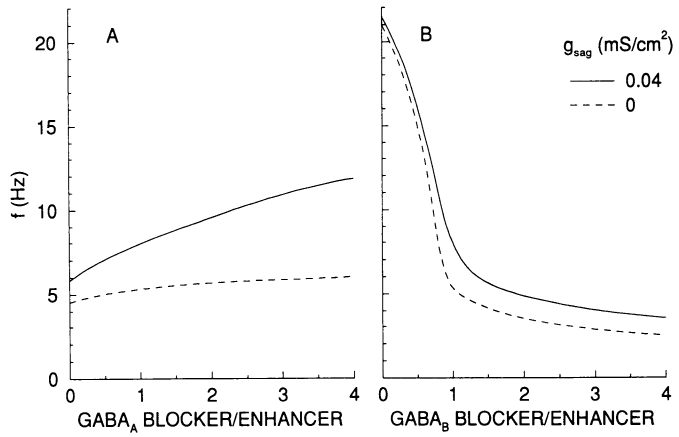

FIG. 12. Dependence of the oscillation frequency on the maximal conductance of $GABA_A$ (A) and $GABA_B$ (B) synapses from RE cells to the TC pool and to other RE cells. Abscissas: ratios between GABA maximal conductances and their corresponding reference values ($g^{RT}_{GABA\text{-}A} = 0.1$ mS/cm^2, $g^{RT}_{GABA\text{-}B} = 0.05$ mS/cm^2, $g_{GABA\text{-}A} = 0.5$ mS/cm^2, $g_{GABA\text{-}B} = 0.1$ mS/cm^2). The ratios $g_{GABA\text{-}A}/g^{RT}_{GABA\text{-}A} = 5$ and $g_{GABA\text{-}B}/g^{RT}_{GABA\text{-}B} = 2$ remain constant. The maximal conductance of the TC pool's sag current (g_{sag}) is = 0.04 mS/cm^2 for the solid curve and 0 for the dashed curve. The rhythmic frequency decreases with enhanced $GABA_B$ inhibition but increases with enhanced $GABA_A$ inhibition. Blockade of the sag current in the TC pool leads to a small change in the $GABA_B$ effect, whereas the effect of $GABA_A$ to increase frequency is strongly reduced but still exists. Changing the maximal conductances from the RE cells to the TC pool without changing the intra-RE coupling yields essentially the same results.

genesis by a strong RE-TC reciprocal connection in the thalamic network.

Steriade's hypothesis and our model

Steriade and colleagues hypothesized that the RE is a generator of spindle rhythmicity (Steriade et al. 1987). Furthermore, they stated that "the RE nucleus is the only factor accounting for the synchronization of spindling activity throughout the thalamus, because there is little, if any, cross-talk between various dorsal thalamic nuclei" (Contreras et al. 1993). Using our model we found that the isolated RE network might indeed oscillate. However, full synchrony was generally not observed in the presence of $GABA_A$ IPSPs, unless the latter's reversal potential was high enough (say less negative than −65 mV). Our results invite a more detailed experimental analysis of the reversal potential for $GABA_A$ inhibition in the RE. Similar results regarding the difficulties in fully synchronizing an RE network were reported by Destexhe et al. (1994a). Our computer simulations showed that partially synchronous oscillations, such as the cluster states, were typically generated by intrinsic synaptic mechanisms in the RE network. In a cluster oscillation state individual cells fire rebound bursts at a lower rate than the population rhythmic frequency; the latter is generally high ($\leq$20 Hz). The fact that the frequency of "spindle waves" observed in the deafferented RE by Steriade et al. (1987) was often in the upper range (14 Hz) and sometimes even higher (15–16 Hz) is consistent with the clustering phenomenon. We suggest that the partial synchrony (clustering) hypothesis could be tested experimentally by computing mean firing rates of single RE cells and comparing them with the field oscillation frequency.

Furthermore, our RE model network was found to be easily synchronized by excitation from the TC pool. Thus our results are consistent with the view of McCormick and colleagues (von Krosigk et al. 1993a) and of Steriade and colleagues (1987) concerning the importance of connections between the RE and relay cells inmaintaining spindle waves. Moreover, rhythmic corticothalamic volleys, impinging during spindling onto RE cells, are also important in facilitating and synchronizing these oscillations.

We emphasize that specific patterns of neuronal population activity generally depend on the values of intrinsic membrane parameters and synaptic inputs as determined by modulating agents. In our model of an isolated RE network, sustained oscillations occur only when the maximal conductance of the T-type Ca^{2+} current and the leakage current take values in appropriate ranges. It is known that neuromodulators, such as acetylcholine or noradrenaline, act on RE cells largely by varying the conductance of a "leak" potassium conductance (McCormick 1992). Serotonin has been found to enhance the T-type Ca^{2+} current in spinal motoneurons (Berger and Takahashi 1990), and might act in a similar manner in thalamic cells. Therefore oscillations in an isolated RE nucleus may be observed in an in vivo preparation only when optimal neuromodulatory conditions are realized. Similarly, in in vitro slice experiments we suggest that a conclusive assessment of whether an isolated RE network is capable of generating its own synchronous oscillations requires a systematic variation of relevant membrane parameters using pharmacological methods.

Partial synchrony of the isolated RE network

When a noiseless and homogeneous RE network oscillates it exhibits a certain degree of synchrony. Neurons are totally asynchronous only if there is a high level of heterogeneity or noise. In the current model synaptic coupling strength between two neurons does not depend on the distance between them, because each neuron is coupled to all the others with the same efficacy. Clustering behavior with such coupling in a system of identical neurons means breaking away spontaneously from uniform behavior to subgroups with different temporal patterns. This is in contrast with symmetry breaking in spatially distributed system, which leads to spatiotemporal patterns (Destexhe et al. 1994a).

Alternating cluster states are characterized by two properties. First, V_{POP} oscillates with a frequency that is 2, 3, or several times faster than the frequency of a single cell. Second, each neuron belongs to a specific group. Each neuron is correlated with others in its group with zero phase shift and with a nonzero phase shift with neurons from other clusters. This property is not preserved under the influence of large noise and sometimes heterogeneity, because neurons shift temporally from one cluster to another. However, such shifting can be observed if the measurement time is smaller than the time characterizing the transitions of neurons between clusters. Because the segregation of neurons into clusters depends on initial conditions and on transient external inputs, any given pair of cells may sometimes be in phase, sometimes out-of-phase. Therefore, we expect that the phase shift in the cross-correlation function between

two given neurons may be nonzero for some initial conditions and zero for others. Different initial conditions can be realized experimentally by briefly stimulating the network and then letting its response relax to the attractor. Fisher et al. (1992) reported from in vivo measurements on rats that cross-correlations between simultaneously recorded RE neurons revealed periods of both in-phase and 180° out-of-phase behaviors. Spontaneous switching between in-phase and out-of-phase oscillations was often seen. More experimental and theoretical work is needed to assess the implications for RE network behavior of the cluster phenomena obtained from our theory.

Patterns similar to these found in our noiseless and homogeneous, isolated RE network (i.e., fully synchronized and cluster oscillations) are reported also in simpler models of coupled RE cells (Golomb and Rinzel 1994b), in models of other neural networks (Ermentrout 1992; Pinsky 1994; Kopell and LeMasson 1994), and in general models of coupled simple oscillator units (for example, see Golomb et al. 1992; Hakim and Rappel 1992; Hansel et al. 1993a,b; Nakagawa and Kuramoto 1993; Schwartz and Tsang 1992; D. Hansel, G. Mato, and C. Meunier, unpublished data) and chaotic maps (Kaneko 1989, 1990). Our partially synchronized patterns are different from those obtained by Kuramoto (1984; Kuramoto and Nishikawa 1987) in simple phase models with heterogeneity. In our system the neurons are well-synchronized with the population voltage, but burst only once in every few cycles. In Kuramoto's system oscillators that are not locked to the population rhythm have different frequencies and cycle asynchronously.

Mechanisms for full synchronization of an RE network

Two mechanisms for fully synchronizing a network of GABAergic neurons are found. One is based on the slowness of the $GABA_B$ inhibition, as discussed in previous works (Wang and Rinzel 1992, 1993; Golomb and Rinzel 1993, 1994a,b). However, this mechanism can be overwhelmed by hyperpolarizing $GABA_A$ IPSPs. It is robust to modest, but not large, amounts of heterogeneity and noise. In addition, the system with $GABA_B$ only oscillates at low frequencies (~5 Hz). When the oscillation frequency is increased, for example by increasing the conductance or the reversal potential of the leak current, the system is less robust to heterogeneity and noise, and at high enough frequency this mechanism does not work at all. Intuitively, if the oscillation frequency is too fast, the $GABA_B$ conductance (rise time 100 ms; decay time 200 ms; Otis et al. 1993) contributes an almost constant inhibition that cannot synchronize the system.

A second mechanism utilizes $GABA_A$ synapses with a less negative reversal potential. The $GABA_A$ conductance then leads to shunting inhibition or even excitation for an important part of the neuron's trajectory. For our parameter values, some $GABA_B$ is also needed to hyperpolarize the neurons and to deinactivate the T-current. However, we cannot exclude the possibility that full synchrony could be realized by shunting $GABA_A$ inhibition in the absence of $GABA_B$ IPSPs, with other parameter choices such as a stronger I_{AHP} or a more negative leak reversal potential. We have observed network oscillations at 4.5–6.5 Hz (Figs. 3*F* and 7, *A* and *C*). Although by changing parameter values we may accelerate somewhat the coherent oscillations, we conclude that the fully synchronized oscillations in our isolated RE network model are limited to a low-frequency range (say <7 Hz), mainly due to the slow time scale of the T-current inactivation at hyperpolarized levels (Huguenard and Prince 1992). It would be of interest to experimentally determine more accurately the reversal potential of $GABA_A$ IPSPs between RE cells and to assess whether the shunting inhibition mechanism discussed here might be relevant to synchronous spindles in the RE network.

Robustness of the fully synchronized oscillations to heterogeneity and noise cannot be increased simply by increasing the synaptic strength; the effects of this increase could even be the opposite. For instance, increasing the $GABA_A$ inhibitory synaptic coupling among neurons reduces the burst duration. When the burst duration is small, noise-induced changes in exact timing reduce the temporal overlap between bursts of different neurons; if the bursts do not overlap at all, the neurons are not synchronous. Similar comments apply to the robustness to heterogeneity.

Another possible mechanism involves the interaction between relay nuclei and the RE. A modest amount of TC-to-RE divergent synaptic excitation was found to synchronize the RE network. In that case the oscillation frequency was sensitive to the coupling strength of the TC-RE reciprocal connection, and could be as high as 20 Hz (see Fig. 12).

Frequency dependence on RE-to-TC inhibition

We have shown that the spindle frequency is sensitive to the $GABA_A$ and $GABA_B$ inhibition from RE to TC cells. As expected, an increase in $GABA_B$ synaptic coupling strength slows the spindle rhythm because the TC pool is hyperpolarized for a prolonged time in every oscillatory cycle. For strong enough $GABA_B$ IPSPs the oscillation frequency remains in the range of 3–5 Hz (Fig. 12*B*). At the same time, increasing the inter-RE $GABA_B$ conductance has little effect on spindle frequency in our model. It is interesting to note that an enhancement of recurrent $GABA_B$ synaptic inhibition has been shown to be capable of triggering petit mal (absence epilepsy) in the thalamic circuitry as an abnormal form of spindle oscillations (Hosford et al. 1992; Liu et al. 1992). The frequency of absence spike-and-wave discharges (~3 Hz in humans, 8 Hz in rats) is lower than that in normal spindles (~10 Hz in humans, 14 Hz in rats). The $GABA_B$-induced frequency decrease that we have found (specific to the RE-to-TC connections) could possibly explain the frequency change that concurs with the transformation from normal spindle oscillations to pathological absence seizure.

On the other hand, surprisingly, enhancing the fast $GABA_A$ inhibition causes the network oscillatory frequency to increase. We explain that phenomenon mainly in terms of the TC pool's sag current kinetic properties. Consistent with our theoretical findings, experimental results of von Krosigk et al. (1993b) showed that blocking $GABA_A$ receptors reduces the frequency of spindle oscillations. However, a word of caution is needed here. The $GABA_A$ effect on our model's oscillation frequency depends on the inactivation property of the sag current during

depolarizing bursts of the TC cells. In the present work the TC cell population is treated as a neuronal pool, which bursts repetitively. In reality, TC cells during spindling fire rebound bursts only occasionally in time, at a much lower rate than the population rhythmic frequency (cf. Steriade et al. 1990). Thus the sag current in individual TC cells should not inactivate strongly in every oscillatory period, and we do not know whether in that situation the $GABA_A$ effect on the oscillation frequency would still occur, possibly as a collective network phenomenon.

Possible consequences of approximations

Despite the fact that the present model is biophysically more realistic than our previous ones (e.g., Golomb and Rinzel 1993, 1994b; Wang and Rinzel 1992, 1993), it still contains several idealizations to make it tractable and consistent with our minimal approach. This approach allows us to dissect the system's dynamics and understand better what are the main factors that affect its behavior. One approximation is that neurons are all-to-all coupled. A randomly partially connected network behaves like an all-to-all network at large $f N$. In reality, the probability that two neurons are coupled decays with the distance between them. Suppose that this decay has a characteristic length λ. We expect that our results on synchronization will be valid for distances of at least λ, but that synchrony between neurons at larger distances may be small. In this case, complex spatiotemporal patterns may emerge (Destexhe et al. 1994a) instead of our cluster oscillations, which are only temporal patterns. Accurate anatomic and physiological data regarding the connectivity are not yet available. Another approximation is introduced by considering the heterogeneity only in g_{Ca}. Effects of heterogeneity in other parameters are presumably similar; the effect of changing many parameters simultaneously would be difficult to interpret. Several simplifications were also made concerning the modeling of single cells. First, the dendritic morphology of the neurons is ignored, as justified by McCormick and Huguenard (1992); however, note that Contreras et al. (1993) reported that RE cells are endowed with an excitable dendritic tree, and dendritic spikes were recorded in 10% of these cells. Second, we have neglected the calcium-activated cation current I_{CAN} (Bal and McCormick 1993). It plays a role in single RE cell behavior like the rebound response on release from hyperpolarization. The slower time scale depolarization of I_{CAN} leads to a finite train of rebound bursts followed by a tail of some sodium spikes. For maintained rhythms, as under study here, the time-averaged or nontransient effects of I_{CAN} may be viewed as incorporated by the leak current. Third, currents for sodium spike generation are also not included in the model. This approximation is not expected to affect the network's behavior on the time scale of bursting ($\sim$100 ms) because the synaptic coupling averages over the fast spikes (which are not expected to be synchronized themselves). Such currents were incorporated in models of single cells (Huguenard and McCormick 1992; McCormick and Huguenard 1992; Rush and Rinzel 1994; Wang 1994) and networks (Destexhe et al. 1994a). By selectively neglecting some of these intrinsic cell properties we obtained a valid and tractable model for studying network rhythmogenesis and burst synchronization at a semiquantitative level. For considering transient behaviors on a faster time scale, or details of a cell's integration of synaptic inputs distributed over the dendritic tree, a description of precise interactions among cells with cable properties would be needed, and therefore further development of models should be important.

RE network as a large dynamic system

In this study we have formulated a biophysical, conductance-based RE network model and then treated it as a large dynamic system. The intrinsic neuronal properties and the synaptic coupling kinetics are expressed as a system of coupled differential equations. This framework enabled us to investigate the long-time behavior of the network in terms of the existence, stability, and basins of attraction of different dynamic patterns. In the current model no geometry is included because the neurons are all-to-all coupled. Despite this fact oscillation patterns in many cases are far from being homogeneous. Therefore models in which the RE is represented by only one cell (Destexhe et al. 1993) should be used with qualification for investigating the cooperative dynamic properties of the RE network. Such models correspond with fully synchronous patterns in our model. The reduced dynamics may be helpful for investigating the dependence of properties of the neuron time courses, such as frequency, on different parameters. However, whether the computed solution is attracting as a homogeneous solution to the network model should be checked. Furthermore, in certain cases stability considerations are not enough, because the system exhibits multistability and the patterns that are selected depend on the relative volume of their basins of attraction. Considering heterogeneity and noise, we have found cases in which the system is fairly robust to heterogeneity and noise and other cases in which it is very sensitive. The active-quiescent cluster state, although an attractive candidate for a synchronized state, is highly sensitive to noise. A small amount of noise can transform it into a state in which all the neurons are well, but not fully, synchronized. In other cases weak noise causes the neurons to burst once in every several periods of the population rhythm.

TC network versus TC pool

In this model the TC cells' output is represented as coming from a single pool. This is a major simplification, because the TC cells are far from being fully synchronized. During spindles the TC cells skip bursts (Steriade et al. 1990; von Krosigk et al. 1993a), and their degree of synchrony is lower than that of the RE cells. However, our main purpose in this paper is to investigate the synchronizing properties of RE cells. Our conclusion that periodic excitation from the TC cells can synchronize the RE network should be valid even if only a subpopulation of TC cells bursts at each period. Because RE cells have overlapping dendritic fields, each one should be receiving a fairly homogeneous excitatory synaptic field from a possibly partially synchronized TC network. The mechanisms that could synchronize a large population of TC cells in the first place are

unaccounted for in the present work. To better understand the dynamics of thalamic spindle oscillations it is important to build a self-consistent model of the coupled RE and TC networks and to consider also the effect of the neocortex on the thalamus. A more elaborated model will have to explain the waxing and waning pattern of spindle oscillations (Steriade et al. 1993).

Despite the fact that the effects of a distributed TC network have not yet been analyzed in our computer simulations, it is interesting to relate the clustering phenomena to in vitro intracellular recordings of a TC cell during spindle oscillations (Figs. 1 and 2 in von Krosigk et al. 1993a). As seen by comparing the intracellular recording with the extracellular one, a TC cell bursts approximately on alternate periods of the population field rhythm, and sometimes it bursts at every third cycle. This TC network possibly exhibits a two-cluster state; noise and heterogeneity could cause neurons to skip bursts and join the other cluster. More generally, however, TC cells burst at even lower rates and remain subthreshold for many of the spindle cycles (cf. Steriade et al. 1990). This kind of clustering phenomena might not be entirely the effect of heterogeneity or noise. A specific cellular property, namely time integration of IPSPs by the intrinsic sag ion current, has been suggested to contribute to such sparse bursting phenomenon in thalamic neurons during spindles (Wang 1994) and in the general context of neural firing patterns (Kopell and LeMasson 1994).

When an RE network oscillates in isolation, the coupling among RE cells determines the network behavior, in particular its synchronization properties. However, when the RE network is coupled to the TC pool, the TC pool can synchronize it even if there is no coupling at all between the RE neurons. Our model network oscillates synchronously when we block all intra-RE synapses. The oscillation frequency does not change significantly (from what is computed in Fig. 12) because it is determined mainly by the excitability of the TC pool. On the other hand, experimental evidence indicates the existence of inhibitory coupling among RE cells (Huguenard and Prince 1993). The role of intra-RE coupling for spindle rhythmogenesis and synchronization can be important if each TC cell is coupled only to a small number of RE cells. Mutual coupling within the RE may also have significance for TC processing in the relay mode. Such questions deserve more experimental study, as well as theoretical study of models of RE and TC networks that take into account the geometry of these nuclei.

We are grateful to J. Chapin, A. Destexhe, D. Hansel, M. Nicolellis, P. Pinsky, and M. Steriade for helpful discussions, and to D. Hansel for a careful reading of this manuscript. We thank J. Huguenard for bringing to our attention the possibility that the reversal potential of $GABA_A$ IPSPs in RE cells may be above −65 mV. We acknowledge computer time provided by the National Cancer Institute Biomedical Supercomputing Center.

Address for reprint requests: D. Golomb, Mathematical Research Branch, NIDDK, National Institutes of Health, 9190 Wisconsin Ave., Suite 350, Bethesda, MD 20814.

Received 25 January 1994; accepted in final form 17 May 1994.

APPENDIX: MODEL EQUATIONS AND PARAMETERS

We use the Hodgkin-Huxley formulation for both the RE cells and the TC pool. Except for the membrane potential V_i, all the other variables that describe an RE cell depend explicitly only on variables of the same cell. For simplicity the index i is omitted in the equations that describe them.

RE cells

Current balance equation

$$C\frac{dV_i}{dt} = -I_{Ca-T}(V_i,h_i) - I_L(V_i) - I_{AHP}(V_i,m_{AHPi}) \quad (A1)$$

$$-I_{GABA-A}(V_i,\{s_{Aj}\}) - I_{GABA-B}(V_i,\{s_{Bj}\}) - I_{AMPA}(V_i,s_P) + C\xi_i(t)$$

$C = 1\ \mu F/cm^2$.

$I_{Ca\text{-}T}$

$$I_{Ca-T}(V,h) = g_{Ca}m_\infty^2(V)h(V - V_{Ca}) \quad (A2)$$

$$\frac{dh}{dt} = \phi(h_\infty(V) - h)/\tau_h(V) \quad (A3)$$

$$m_\infty(V) = [1 + \exp(-(V - \theta_m)/\sigma_m)]^{-1} \quad (A4)$$

$$h_\infty(V) = [1 + \exp(-(V - \theta_h)/\sigma_h)]^{-1} \quad (A5)$$

$$\tau_h(V) = 100 + 500 \times [1 + \exp(-(V - \theta_{ht})/\sigma_{ht})]^{-1} \quad (A6)$$

$g_{Ca} = 2\ mS/cm^2$, $V_{Ca} = 120$ mV, $\theta_m = -52$ mV, $\sigma_m = 7.4$ mV, $\theta_h = -78$ mV, $\sigma_h = -5$ mV, $\theta_{ht} = -78$ mV, $\sigma_{ht} = -3$ mV, $\phi = 4.2$ (Huguenard and Prince 1992).

An estimate of g_{Ca} is obtained from the whole-cell voltage-clamp data of Huguenard and Prince (1992). In their Fig. 3*B* the voltage-pulse-elicited T-type current has a measured peak of ~0.21 nA. By using *Eq. A2* and substituting $m_\infty \approx 1$, $h \approx 1$, and $V - V_{Ca} = 120$ mV, the measured current maximum can be matched with $g_{Ca} \times$ cell area $= 1.6 \times 10^{-12}$ S. Approximating the RE neuron by a sphere with a 30 μm diam (Steriade et al. 1990) yields $g_{Ca} = 0.6\ mS/cm^2$. This estimate is rough because some of the calcium channels are likely located in dendrites (Contreras et al. 1993). As our reference parameter we chose $g_{Ca} = 2\ mS/cm^2$ to produce oscillations.

I_L

$$I_L = g_L(V - V_L) \quad (A7)$$

$g_{LR} = 0.06\ mS/cm^2$, $V_L = -60$ mV (Avanzini et al. 1989).

I_{AHP}: the kinetic properties of this current in RE cells have not been experimentally determined. We utilize a simple expression of I_{AHP} similar to that in Yamada et al. (1989) but with faster kinetics (Destexhe et al. 1993, 1994a)

$$I_{AHP}(V, m_{AHP}) = g_{AHP}m_{AHP}(V - V_K) \quad (A8)$$

$$\frac{d[Ca]}{dt} = -\nu I_{Ca-T} - \gamma[Ca] \quad (A9)$$

$$\frac{dm_{AHP}}{dt} = \alpha[Ca](1 - m_{AHP}) - \beta m_{AHP} \quad (A10)$$

$g_{AHP} = 0.3\ mS/cm^2$, $V_K = -90$ mV, $\alpha = 0.02\ ms^{-1}$, $\beta = 0.025\ ms^{-1}$, $\nu = 0.0\ 1\ ms^{-1}$, $\gamma = 0.08\ ms^{-1}$.

$I_{GABA\text{-}A}$

$$I_{GABA-A}(V, \{s_{Aj}\}) = g_{GABA-A}(V - V_{GABA-A})\frac{1}{N}\sum_{j=1}^{N} s_{Aj} \quad (A11)$$

$$\frac{ds_{Aj}}{dt} = k_{fA}x_\infty(V_j)(1 - s_{Aj}) - k_{rA}s_{Aj} \quad (A12)$$

$$x_\infty(V) = [1 + \exp(-(V - \theta_s)/\sigma_s)]^{-1} \quad (A13)$$

where V_j is the presynaptic membrane potential. $\theta_s = -45$ mV, $\sigma_s = 2$ mV (for both $GABA_A$ and $GABA_B$), $g_{GABA\text{-}A} = 0.5\ mS/cm^2$, $V_{GABA\text{-}A} = -75$ mV, $k_{fA} = 2.0\ ms^{-1}$, and $k_{rA} = 0.08\ ms^{-1}$. This representation of synaptic current was developed by Wang and Rinzel (1992, 1993) and Destexhe et al. (1994b). For the kinetics of $GABA_A$ see Otis and Mody (1992) and Ropert et al. (1990).

$I_{\text{GABA-B}}$

$$I_{\text{GABA-B}}(V, \{s_{\text{Bj}}\}) = g_{\text{GABA-B}}(V - V_{\text{GABA-B}}) \frac{1}{N} \sum_{j=1}^{N} s_{\text{Bj}} \quad (A14)$$

$$\frac{dx_{\text{Bj}}}{dt} = k_{\text{fx}} x_{\infty}(V_j)(1 - x_{\text{Bj}}) - k_{\text{rx}} x_{\text{Bj}} \quad (A15)$$

$$\frac{ds_{\text{Bj}}}{dt} = k_{\text{fB}} s_{\infty}(x_{\text{Bj}})(1 - s_{\text{Bj}}) - k_{\text{rB}} s_{\text{Bj}} \quad (A16)$$

$$s_{\infty}(x_{\text{B}}) = [1 + \exp(-(x_{\text{B}} - 1/e)/0.02)]^{-1} \quad (A17)$$

$g_{\text{GABA-B}} = 0.1$ mS/cm^2, $V_{\text{GABA-B}} = -90$ mV, $k_{\text{fx}} = 5.0$ ms^{-1}, $k_{\text{rx}} = 0.01$ ms^{-1}, $k_{\text{fB}} = 0.01$ ms^{-1}, and $k_{\text{rB}} = 0.005$ ms^{-1}. Note that we have introduced an auxiliary variable x_{B} to model the slow rise in GABA_{B} conductance. *Equation A15* with $k_{\text{fx}} \gg k_{\text{rx}}$ implies that x_{B} is activated by a brief presynaptic pulse very rapidly, then decays at a finite rate k_{rx}. It thus stays above the value of $1/e$ for a time interval of $\sim 1/k_{\text{rx}}$. According to *Eq. A16*, during the time when x_{B} is above $1/e$, the synaptic variable s_{B} increases; thus its rise time is given by $1/k_{\text{rx}}$ (note that $k_{\text{fB}} = k_{\text{rx}}$). Later, s_{B} decays with a time constant $1/k_{\text{rB}}$. The synaptic conductance mimics the GABA_{B} kinetics measured by Otis et al. (1993).

AMPA current I_{AMPA}

$$I_{\text{AMPA}}(V, s_{\text{P}}) = g_{\text{AMPA}}(V - V_{\text{AMPA}}) s_{\text{P}} \quad (A18)$$

$g_{\text{AMPA}} = 0.1$ mS/cm^2, $V_{\text{AMPA}} = 0$ mV. The gating variable s_{P} depends on the membrane potential of the TC pool, and its kinetic equation is given below (*Eq. A35* and *A36*).

Heterogeneity: g_{Ca} is assigned from a uniform distribution $\rho(g_{\text{Ca}})$ (Golomb and Rinzel 1993)

$$\rho(g_{\text{Ca}}) = \begin{cases} \dfrac{1}{2\sqrt{3}\sigma_{\text{g}}} & \bar{g}_{\text{Ca}} - \sqrt{3}\sigma_{\text{g}} \le g_{\text{Ca}} \le \bar{g}_{\text{Ca}} + \sqrt{3}\sigma_{\text{g}} \\ 0 & \text{otherwise,} \end{cases} \quad (A19)$$

whose mean is $\bar{g}_{\text{Ca}} = 2$ mS/cm^2.

Noise: $\xi_i(t)$ is white, Gaussian, and local (different from neuron to neuron)

$$\langle \xi_i(t) \rangle = 0 \quad (A20)$$

$$\langle \xi_i(t) \xi_j(t') \rangle = 2D\delta_{ij}\delta(t - t') \quad (A21)$$

where $\langle \ldots \rangle$ denotes average over realizations (Golomb and Rinzel 1994b).

Tc pool

The parameters of the TC pool (representative "neuron") were chosen such that the "cell" bursts at every time period when coupled to the RE cells. This pool idealizes a population of TC cells, each of which usually burst only once in every few population cycles (Steriade et al. 1990, von Krosigk et al. 1993a). All the variables, expressions, and parameters from now on are related to the TC pool unless stated differently.

Current balance equation

$$C \frac{dV}{dt} = -I_{\text{Ca-T}}(V, h) - I_{\text{L}}(V) - I_{\text{sag}}(V, r) \quad (A22)$$

$$- I^{RT}_{\text{GABA-A}}(V, \{s_{\text{Aj}}\}) - I^{RT}_{\text{GABA-B}}(V, \{s_{\text{Bj}}\})$$

$C = 1\ \mu\text{F/cm}^2$.

$I_{\text{Ca-T}}$

$$I_{\text{Ca-T}}(V, h) = g_{\text{Ca}} m^2_{\infty}(V) h (V - V_{\text{Ca}}) \quad (A23)$$

$$\frac{dh}{dt} = \phi(h_{\infty}(V) - h)/\tau_{\text{h}}(V) \quad (A24)$$

$$m_{\infty}(V) = [1 + \exp(-(V - \theta_{\text{m}})/\sigma_{\text{m}})]^{-1} \quad (A25)$$

$$h_{\infty}(V) = [1 + \exp(-(V - \theta_{\text{h}})/\sigma_{\text{h}})]^{-1} \quad (A26)$$

$$\tau_{\text{h}}(V) = 30 + 220 \times [1 + \exp(-(V - \theta_{\text{ht}})/\sigma_{\text{ht}})]^{-1} \quad (A27)$$

$g_{\text{Ca}} = 2.5$ mS/cm^2, $V_{\text{Ca}} = 120$ mV, $\theta_{\text{m}} = -59$ mV, $\sigma_{\text{m}} = 6.2$ mV, $\theta_{\text{h}} = -81$ mV, $\sigma_{\text{h}} = -4.4$ mV, $\theta_{\text{ht}} = -78$ mV, $k_{\text{ht}} = -3$ mV, and $\phi = 4.2$ (Huguenard and McCormick 1992).

I_{L}

$$I_{\text{L}} = g_{\text{L}}(V - V_{\text{L}}) \quad (A28)$$

$g_{\text{L}} = 0.025$ mS/cm^2, $V_{\text{L}} = -75$ mV. This represents a combination of a sodium leak current (with a reversal potential of +45 mV) and a potassium leak current (with a reversal potential of −105 mV) (McCormick and Huguenard 1992).

I_{sag}

$$I_{\text{sag}}(V, r) = g_{\text{sag}} r (V - V_{\text{sag}}) \quad (A29)$$

$$\frac{dr}{dt} = (r_{\infty}(V) - r)/\tau_{\text{sag}}(V) \quad (A30)$$

$$r_{\infty}(V) = [1 + \exp(-(V - \theta_{\text{sag}})/\sigma_{\text{sag}})]^{-1} \quad (A31)$$

$$\tau_{\text{sag}}(V) = 20 + 1000/[\exp((V + 71.5)/14.2) + \exp(-(V + 89.0)/11.6)] \quad (A32)$$

$g_{\text{sag}} = 0.04$ mS/cm^2, $V_{\text{sag}} = -40.0$ mV, $\theta_{\text{sag}} = -75$ mV, $\sigma_{\text{sag}} = -5.5$ mV (Huguenard and McCormick 1992).

The isolated TC pool is also a conditional oscillator. It is at rest with our reference parameter set, but oscillates at low frequency (2–3 Hz) for more negative values of the leak reversal potential. These endogenous oscillations in the delta frequency range are created by an interplay between the T-type Ca^{2+} current and the hyperpolarization-activated cation ("sag") current (Leresche et al. 1991; McCormick and Pape 1990).

$I^{RT}_{GABA\text{-}A}$ from RE cells to TC pool

$$I^{RT}_{GABA-A}(V, \{s_{\text{Aj}}\}) = g^{RT}_{\text{GABA-A}}(V - V_{\text{GABA-A}}) \frac{1}{N} \sum_{j=1}^{N} s_{\text{Aj}} \quad (A33)$$

$g^{RT}_{GABA\text{-}A} = 0.1$ mS/cm^2; see *Eq. A12* and *A13*.

$I^{RT}_{GABA\text{-}B}$ from RE cells to TC pool

$$I^{RT}_{\text{GABA-A}}(V, \{s_{\text{Bj}}\}) = g^{RT}_{\text{GABA-B}}(V - V_{\text{GABA-B}}) \frac{1}{N} \sum_{j=1}^{N} s_{\text{Bj}} \quad (A34)$$

$g^{RT}_{GABA\text{-}B} = 0.05$ mS/cm^2; see *Eq. A15–A17*.

AMPA gating variable

$$\frac{ds_{\text{P}}}{dt} = k_{\text{fP}} s_{\infty}(\text{V})(1 - s_{\text{P}}) - k_{\text{rP}} s_{\text{P}} \quad (A35)$$

$$s_{\infty}(V) = [1 + \exp(-(V - \theta_{\text{s}})/\sigma_{\text{s}})]^{-1} \quad (A36)$$

$\theta_{\text{s}} = -45$ mV, $\sigma_{\text{s}} = 2$ mV, $k_{\text{fP}} = 2.0$ ms^{-1}, and $k_{\text{rP}} = 0.1$ ms^{-1}. We use the formulation of Wang and Rinzel (1993) and estimate parameters on the basis of the experimental data of Stern et al. (1992) and McBain and Dingledine (1992). Changing the decay time of GABA_{A} and AMPA synapses by a factor of 2 does not have any significant effect on the results, because these decay times are much faster than the oscillation period. In most cases even assuming these synapses as instantaneous is a very good approximation.

REFERENCES

ABBOTT, L. F. AND VAN VREESWIJK, C. Asynchronous states in networks of pulse-coupled oscillators. *Phys. Rev.* E48: 1483–1490, 1993.

ANDERSEN, P. AND ANDERSSON, S. A. *Physiological Basis of the Alpha Rhythm.* New York: Appleton-Century-Crofts, 1968.

AVANZINI, G., DE CURTIS, M., PANZICA, F., AND SPREAFICO, F. Intrinsic properties of nucleus reticularis thalami neurons of the rat studied in vitro. *J. Physiol. Lond.* 416: 111–122, 1989.

BACK, A., GUCKENHEIMER, J., MYERS, M., WICKLIN, F., AND WORFOLK, P. Dstool: computer assisted exploration of dynamical systems. *N. Am. Math. Soc.* 39: 303–309, 1992.

BAL, T. AND MCCORMICK, D. A. Mechanisms of oscillatory activity in guinea-pig nucleus reticularis thalami in vitro: a mammalian pacemaker. *J. Physiol. Lond.* 468: 669–691, 1993.

BERGÉ, P., POMEAU, Y., AND VIDEL, C. *Order Within Chaos.* New York: Wiley, 1984.

BERGER, A. J. AND TAKAHASHI, T. Serotonin enhances a low-activated calcium current in rat spinal motoneurons. *J. Neurosci.* 10: 1922–1928, 1990.

BUZSÁKI, G. The thalamic clock: emergent network properties. *Neuroscience* 41: 351–364, 1991.

CONTRERAS, D., CURRÓ DOSSI, R., AND STERIADE, M. Electrophysiological properties of cat reticular thalamic neurons in vivo. *J. Physiol. Lond.* 470: 273–394, 1993.

COULTER, D. A., HUGUENARD, J. R., AND PRINCE, D. A. Calcium current in rat thalamocortical relay neurons: kinetic properties of the transient, low threshold current. *J. Physiol. Lond.* 414: 587–604, 1989.

DESCHÊNES, M., MADARIAGA-DOMICH, A., AND STERIADE, M. Dendrodendritic synapses in the cat reticularis thalami nucleus: a structural basis for thalamic spindle synchronization. *Brain Res.* 334: 165–168, 1985.

DESCHÊNES, M., PARADIS, M., ROY, J. P., AND STERIADE, M. Electrophysiology of neurons of lateral thalamic nuclei in rat: resting properties and burst discharges. *J. Neurophysiol.* 51: 1196–1219, 1984.

DESTEXHE, A., CONTRERAS, D., SEJNOWSKI, T. J., AND STERIADE, M. A model of spindle rhythmicity in the isolated thalamic reticular nucleus. *J. Neurophysiol.* 72: 803–818, 1994a.

DESTEXHE, A., MAINEN, Z., AND SEJNOWSKI, T. J. An effective method for computing synaptic conductance based on a kinetic model of receptor binding. *Neural Comput.* 6: 14–18, 1994b.

DESTEXHE, A., MCCORMICK, D. A., AND SEJNOWSKI, T. J. A model for 8–10 Hz spindling in interconnected thalamic relay and reticularis neurons. *Biophys. J.* 65: 2473–2477, 1993.

ERMENTROUT, G. B. Complex dynamics in winner-take-all neural nets with slow inhibition. *Neural Networks* 5: 415–431, 1992.

FISHER, T. M., NICOLELLIS, M. A. L., AND CHAPIN, J. K. Sensory and oscillatory properties of simultaneously recorded multi-single units in the thalamic reticular nucleus of the rat. *Soc. Neurosci. Abstr.* 18: 1392, 1992.

GOLOMB, D., HANSEL, D., SHRAIMAN, B., AND SOMPOLINSKY, H. Clustering in globally coupled phase oscillators. *Physiol. Rev.* A45: 3516–3530, 1992.

GOLOMB, D. AND RINZEL, J. Dynamics of globally coupled inhibitory neurons with heterogeneity. *Physiol. Rev.* E48: 4810–4814, 1993.

GOLOMB, D. AND RINZEL, J. Synchronization among heterogeneous inhibitory RTN neurons globally coupled. In: *Computation in Neurons and Neural Systems,* edited by F. H. Eeckman. Boston, MA: Kluwer, 1994a, p. 27–32.

GOLOMB, D. AND RINZEL, J. Clustering in globally coupled inhibitory neurons. *Physica* D72: 259–282, 1994b.

GOLOMB, D., WANG, X.-J., AND RINZEL, J. Synchronization among GABAergic neurons in a globally coupled network. *Soc. Neurosci. Abstr.* 19: 1584, 1993.

GUCKENHEIMER, J. AND HOLMES, P. *Nonlinear Oscillations, Dynamical Systems, and Bifurcations of Vector Fields.* Berlin: Springer-Verlag, 1983.

HAKIM, V. AND RAPPEL, W. J. Dynamics of the globally coupled complex Ginzburg-Landau equation. *Physiol. Rev.* A46: 7347–7350, 1992.

HANSEL, D., MATO, G., AND MEUNIER, C. Clustering and slow switching in globally coupled phase oscillators. *Physiol. Rev.* E48: 3470–3477, 1993a.

HANSEL, D., MATO, G., AND MEUNIER, C. Phase reduction and neural modeling. Functional analysis of the brain based on multiple-site recordings. *Concepts Neurosci.* 4: 192–210, 1993b.

HANSEL, D. AND SOMPOLINSKY, H. Synchronization and computation in a chaotic neural network. *Physiol. Rev. Lett.* 89: 718–721, 1992.

HOSFORD, D. A., CLARK, S., CAO, Z., WILSON, W. A., JR., LIN, F.-H., MORRISETT, R. A., AND HUIN, A. The role of $GABA_B$ receptor activation in absence seizure of lethargic (*lh/lh*) mice. *Science Wash. DC* 257: 398–401, 1992.

HOUSER, C. R., VAUGHAN, J. E., BARBER, R. P., AND ROBERTS, E. GABA neurons are the major cell type of the nucleus reticularis thalami. *Brain Res.* 200: 341–354, 1980.

HUGUENARD, J. R. AND MCCORMICK, D. A. Simulation of the currents involved in rhythmic oscillations in thalamic relay neurons. *J. Neurophysiol.* 68: 1373–1383, 1992.

HUGUENARD, J. R. AND PRINCE, D. A. A novel T-type current underlies prolonged Ca^{2+}–dependent burst firing in GABAergic neurons of rat thalamic reticular nucleus. *J. Neurosci.* 12: 3804–3817, 1992.

HUGUENARD, J. R. AND PRINCE, D. A. Clonazepam suppresses $GABA_B$ inhibition in relay cells through actions in the reticular nucleus. *Soc. Neurosci. Abstr.* 19: 1704, 1993.

JAHNSEN, H. AND LLINÁS, R. R. Electrophysiological properties of guinea-pig thalamic neurons: an in vitro study. *J. Physiol. Lond.* 349: 205–226, 1984a.

JAHNSEN, H. AND LLINÁS, R. R. Ionic basis for the electroresponsiveness and oscillatory properties of guinea-pig thalamicneurons in vitro. *J. Physiol. Lond.* 349: 227–247, 1984b.

KANEKO, K. Chaotic but regular posi-nega switch among coded attractors by cluster-size variation. *Physiol. Rev. Lett.* 63: 219–223, 1989.

KANEKO, K. Clustering, coding, switching, hierarchal ordering, and control in a network of chaotic elements. *Physica* D41: 137–172, 1990.

KOPELL, N. AND LEMASSON, G. Rhythmogenesis, amplitude modulation and multiplexing in a cortical architecture. *Proc. Natl. Acad. Sci.* USA. In press.

KURAMOTO, Y. *Chemical Oscillations, Waves and Turbulence.* New York: Springer-Verlag, 1984.

KURAMOTO, Y. AND NISHIKAWA, I. Statistical macrodynamics of large dynamical systems. Case of a phase transition in oscillator communities. *J. Stat. Phys.* 49: 569–605, 1987.

LERESCHE, N., LIGHTOWLER, S., SOLTESZ, I., JASSIK-GERSCHENFELD, D., AND CRUNELLI, V. Low-frequency oscillatory activities intrinsic to cat and rat thalamocortical cells. *J. Physiol. Lond.* 441: 155–174, 1991.

LIU, Z., VERGNES, M., DEPAULIS, A., AND MARESCAUX, C. Involvement of intrathalamic $GABA_B$ neurotransmission in the control of absence seizures in the rat. *Neuroscience* 48: 87–93, 1992.

LLINÁS, R. R. AND GEIJO-BARRIENTOS, E. In vitro studies of mammalian thalamic and reticularis thalami neurons. In: *Cellular Thalamic Mechanisms,* edited by M. Bentivoglio and R. Spreafico. Amsterdam: Elsevier, 1988, p. 23–33.

MCBAIN, C. J. AND DINGLEDINE, R. Dual-component miniature excitatory synaptic currents in rat hippocampal CA3 pyramidal neurons. *J. Neurophysiol.* 68: 16–27, 1992.

MCCORMICK, D. A. Neurotransmitter actions in the thalamus and cerebral cortex and their role in neuromodulation of thalamocortical activity. *Prog. Neurobiol.* 39: 337–388, 1992.

MCCORMICK, D. A. AND HUGUENARD, J. R. A model of the electrophysiological properties of thalamocortical relay neurons. *J. Neurophysiol.* 68: 1384–1400, 1992.

MCCORMICK, D. A. AND PAPE, H.-C. Properties of a hyperpolarization activated cation current and its role in rhythmic oscillation in thalamic relay neurons. *J. Physiol. Lond.* 431: 291–318, 1990.

MONTERO, V. M. AND SINGER, W. Ultrastructure and synaptic relations of neural elements containing glutamic acid decarboxylase (GAD) in the perigeniculate nucleus of the cat. *Exp. Brain Res.* 56: 115–125, 1984.

MULLE, C., MADARIAGA, A., AND DESCHÊNES, M. Morphology and electrophysiological properties of reticularis thalami neurons in cat: in vivo study of a thalamic pacemaker. *J. Neurosci.* 6: 2134–2145, 1986.

MULLE, C., STERIADE, M., AND DESCHÊNES, M. Absence of spindle oscillations in the cat anterior thalamic nuclei. *Brain Res.* 334: 169–171, 1985.

NAKAGAWA, N. AND KURAMOTO, Y. Collective chaos in a population of globally coupled oscillators. *Prog. Theor. Phys.* 89: 313–323, 1993.

OHARA, P. T. AND LIEBERMAN, A. L. The thalamic reticular nucleus of the adult rat: experimental anatomical studies. *J. Neurocytol.* 14: 365–411, 1985.

OTIS, T. S., DE KONINK, Y. D., AND MODY, I. Characterization of synaptically elicited $GABA_B$ responses using patch-clamp recordings in rat hippocampal slices. *J. Physiol. Lond.* 463: 391–407, 1993.

OTIS, T. S. AND MODY, I. Modulation of decay kinetics and frequency of $GABA_A$ receptor-mediated spontaneous inhibitory postsynaptic currents in hippocampal neurons. *Neuroscience* 49: 13–32, 1992.

PINSKY, P. F. *Mathematical Models of Hippocampal Neurons and Neural Networks: Exploiting Multiple Time Scales* (PhD thesis). College Park, MD: Univ. of Maryland, 1993.

PINSKY, P. F. Synchrony and clustering in an excitatory neural network model with intrinsic relaxation kinetics. *SIAM J. Appl. Math.* In press.

RINZEL, J. AND ERMENTROUT, G. B. Analysis of neural excitability and oscillations. In: *Methods in Neuronal Modeling,* edited by C. Koch and I. Segev. Cambridge, MA: MIT Press, 1989, p. 135–169.

ROPERT, N., MILES, R., AND KORN, H. Characteristics ofminiature inhibitory postsynaptic currents in CA1 pyramidal neurons of rathippocampus. *J. Physiol. Lond.* 428: 707–722, 1990.

RUSH, M. E. AND RINZEL, J. Analysis of bursting in a thalamic neuron model. *Biol. Cybern.* In press.

SCHWARTZ, I. B. AND TSANG, K. Y. Predicting attracting out-of-phase states in coupled Josephson junctions. *Int. J. Bifurcation Chaos* 1: 177–181, 1992.

SHOSAKU, A., KAYAMA, Y., SUMITOMO, I., SUGITANI, M., AND IWAMA, K. Analysis of recurrent inhibitory circuit in rat thalamus: neurophysiology of the thalamic reticular nucleus. *Prog. Neurobiol.* 32: 77–102, 1989.

SPREAFICO, R., DE CURTIS, M., FRASSONI, C., AND AVANZINI, G. Electrophysiological characteristics of morphologically identified reticular thalamic neurons from rat slices. *Neuroscience* 27: 629–638, 1988.

STERIADE, M. AND DESCHÊNES, M. The thalamus as a neuronal oscillator. *Brain Res. Rev.* 8: 1–63, 1984.

STERIADE, M., DESCHÊNES, M., DOMICH, L., AND MULLE, C. Abolition of spindle oscillations in thalamic neurons disconnected from nucleus reticularis thalami. *J. Neurophysiol.* 54: 1473–1497, 1985.

STERIADE, M., DOMICH, L., OAKSON, G., AND DESCHÊNES, M. The deafferented reticularis thalami nucleus generates spindle rhythmicity. *J. Neurophysiol.* 57: 260–273, 1987.

STERIADE, M., JONES, E. G., AND LLINÁS, R. R. *Thalamic Oscillations and Signaling.* New York: Wiley, 1990.

STERIADE, M., MCCORMICK, D. A., AND SEJNOWSKI, T. J. Thalamocortical oscillations in the sleeping and aroused brain. *Science Wash. DC* 262: 679–685, 1993.

STERN, P., EDWARDS, F. A., AND SAKMANN, B. Fast and slow components of unitary EPSPs on stellate cells elicited by focal stimulation in slices of rat visual cortex. *J. Physiol. Lond.* 449: 247–278, 1992.

VAN KAMPEN, N. G. *Stochastic Processes in Physics and Chemistry.* Amsterdam: North-Holland, 1981.

VON KROSIGK, M., BAL, T., AND MCCORMICK, D. A. Cellular mechanisms of a synchronized oscillation in the thalamus. *Science Wash. DC* 261: 361–364, 1993a.

VON KROSIGK, M., BAL, T., AND MCCORMICK, D. A. Cellular mechanisms of thalamic synchronized oscillations in thalamocortical relay neurons. *Soc. Neurosci. Abstr.* 19: 528, 1993b.

WANG, X.-J. Multiple dynamical modes of thalamic relay neurons: rhythmic bursting and intermittent phase-locking. *Neuroscience* 59: 21–31, 1994.

WANG, X.-J. AND RINZEL, J. Alternating and synchronous rhythms in reciprocally inhibitory model neurons. *Neural Comput.* 4: 84–97, 1992.

WANG, X.-J. AND RINZEL, J. Spindle rhythmicity in the reticularis thalami nucleus: synchronization among mutually inhibitory neurons. *Neuroscience* 53: 899–904, 1993.

WANG, X.-J., RINZEL, J., AND ROGAWSSKI, M. A. A model of the T-type calcium current and the low threshold spike in thalamic neurons. *J. Neurophysiol.* 66: 839–850, 1991.

YAMADA, W., KOCH, C., AND ADAMS, P. R. Multiple channels and calcium dynamics. In: *Methods in Neuronal Modeling,* edited by C. Koch and I. Segev. Cambridge, MA: MIT Press, 1989, p. 97–133.

YEN, C. T., CONLEY, M., HENDRY, H. C., AND JONES, E. G. The morphology of physiologically identified GABAergic neurons in the somatic sensory part of the thalamic reticular nucleus in the cat. *J. Neurosci.* 5: 2254–2268, 1985.